ELSEVIER

Contents lists available at ScienceDirect

Matrix Biology

journal homepage: www.elsevier.com/locate/matbio





Fibrolamellar carcinomas–growth arrested by paracrine signals complexed with synthesized 3-O sulfated heparan sulfate oligosaccharides *, * **

Wencheng Zhang a,b,c,d,1 , Yongmei Xu e,f,1,2 , Xicheng Wang b,c,d,3 , Tsunekazu Oikawa a , Guowei Su f , Eliane Wauthier a , Guoxiu Wu b,c,d , Praveen Sethupathy g,4 , Zhiying He b,c,d,3,4,6 , Jian Liu e,f,2,4,5 , Lola M. Reid a,h,4,7,*

- ^a Department of Cell Biology and Physiology, University of North Carolina, Chapel Hill, NC 27599, United States
- b Institute for Regenerative Medicine, Shanghai East Hospital, School of Life Sciences and Technology, Tongii University School of Medicine, Shanghai 200123, China
- ^c Shanghai Engineering Research Center of Stem Cells Translational Medicine, Shanghai 200335, China
- ^d Shanghai Institute of Stem Cell Research and Clinical Translation, Shanghai 200120, China
- e Division of Chemical Biology and Medicinal Chemistry, Eshelman School of Pharmacology, University of North Carolina, Chapel Hill, NC 27599, United States
- f Glycan Therapeutics Corporation, 617 Hutton Street, Raleigh, NC 27606, United States
- ^g Division of Biomedical Sciences, College of Veterinary Medicine, Cornell University, Ithaca, NY 14853, United States
- h Program in Molecular Biology and Biotechnology, School of Medicine, University of North Carolina, Chapel Hill, NC 27599, United States

Abbreviations: ABs, angioblasts (CD117+, VEGFr+, CD133+, CD31+) and their descendants, precursors to endothelia (VEGFr+, CD133+, CD31+) and to stellate cells (CD146⁺, ICAM-1⁺, vitamin A'); AFP, α-fetoprotein; ALB, albumin; ALDHs, aldehyde dehydrogenases; BTSCs, biliary tree stem cell subpopulations; CD, common determinant; CD44, hyaluronan receptors; CD133, prominin; CFTR, cystic fibrosis transmembrane conductance regulator; CK, cytokeratin protein; CXCR4, CXCchemokine receptor 4 (also called fusin or CD184 also called platelet factor 4; EGF, epidermal growth factor; EpCAM, epithelial cell adhesion molecule; FGF, fibroblast growth factor; Fzd, Frizzled proteins are seven transmembrane receptors that can respond to Wnt proteins to activate the canonical β-catenin pathway; GAGs, glycosaminoglycans, polymers of the disaccharide unit, [uronic acid and an amino sugar]N; GlcA, β-D-glucuronic acid; GlcNAc, N-acetylated glucosamine; GlcNS, 2-deoxy-2-sulfamido-α-D-glucopyranosyl; GlcNS(6S), 2-deoxy-2-sulfamido-α-D-glucopyranosyl-6-O-sulfate; HA, hyaluronans, non-sulfated, anionic polymers of the disaccharide unit, [glucuronic acid- n-acetylglucosamine]N; IdoA, \(\alpha \)-L-iduronic acid; IdoA(2S), 2-O-sulfo-\(\alpha \)-L-iduronic acid; HBs, hepatoblasts; HGF, hepatocyte growth factor; HPs, Heparins, highly sulfated polymers of the disaccharide unit [glucronic acid-glucosamine]_N; HRs, heparosan, a non-sulfated polymer of the disaccharide unit: [β-D-glucuronic acid-N-acetyl-α-D-glucosamine]_N; HpSCs, hepatic stem cells; HS, heparan sulfates, variably sulfated polymers of glucuronic acidglucosamine; HS polymerase, heparan sulfate polymerase needed to synthesize the backbone of the polysaccharide for HSs and HPs; HS-PG, heparan sulfate proteoglycan; ICAM-1, intercellular cell adhesion molecule and one of surface molecules to which HAs bind; KLF4/KLF5, Krüppel-like factors 4 or 5, zinc finger proteins that are transcription factors in stem cells; KM, Kubota's Medium, a serum-free medium designed for endodermal stem cells; KRT, cytokeratin gene; LGR5, Leucinerich repeat-containing G-protein coupled receptor 5 that binds to R-spondin; MMPs, matrix metalloproteinases; NDST, N-deacetylase/ N-sulfotransferase; NANOG, a transcription factor critically involved with self-renewal; NCAM, neural cell adhesion molecule; NIS, sodium/iodide symporter; OCT4, octamer-binding transcription factor 4 also known as POU5F1 (POU domain, class 5, transcription factor 1), a gene expressed by stem cells; PBGs, peribiliary glands, stem cell niches for biliary tree stem cells; PDX1, pancreatic and duodenal homeobox 1, a transcsription factor critical for pancreatic development; PSCs, pancreatic stem cells; SALL4, Sal-like protein 4 found to be important for self-replication of stem cells; SOX, Sry-related HMG box; SOX2, a transcription factor that is essential for maintaining self-renewal, or pluripotency in embryonic and determined stem cells; SOX9, transcription factor associated with liver, pancreas and intestine; SOX17, a transcription factor essential for differentiation of liver; VEGF, vascular endothelial cell growth factor; Wnt, Wingless-type MMTV integration site family.

https://doi.org/10.1016/j.matbio.2023.06.008

Received 29 March 2023; Received in revised form 30 May 2023; Accepted 28 June 2023 Available online 2 July 2023

0945-053X/© 2023 The Authors. Published by Elsevier B.V. This is an open access article under the CC BY-NC-ND license (http://creativecommons.org/licenses/by-nc-nd/4.0/).

^{*} Senior Authors. The senior authors handled management for the experimental studies and for the funding. The senior corresponding authors were responsible for the studies presented in this manuscript and for all drafts of the manuscript. ** Acronyms for cell populations (or for names of antibodies derived from a specific species) are preceded by a small letter to indicate the species: *m*=murine; *h*=human; *r*=rabbit; *g*=goat; *d*=donkey.

^{*} Corresponding author.

E-mail address: stemcell@med.unc.edu (L.M. Reid).

¹ First Authors: The first authors were responsible for managing the key facets of the benchwork in the experiments in biliary tree/hepatic stem cell biology and their regulation by complexes of heparan sulfate oligosaccharides and paracrine signals.

² In the preparation of the synthesized glycosaminoglycans.

³ In the bioinformatics and for preparation of all drafts of the manuscript.

⁴ Senior Authors: The senior authors handled management for the experimental studies and for the funding. The senior corresponding authors were responsible for the studies presented in this manuscript and for all drafts of the manuscript. Praveen Sethupathy, PhD. Department of Biomedical Sciences, College of Veterinary Medicine, Cornell University Veterinary Research Tower T7 006D, Ithaca, NY 14853. Email: pr46@cornell.edu Phone: 607–253–4347.

ARTICLE INFO

Keywords: Fibrolamellar carcinomas, Biliary tree stem cells (hepato/pancreatic stem cells) Organoids Paracrine signals Synthesized heparan sulfate oligosaccharides

ABSTRACT

Fibrolamellar carcinomas (FLCs), lethal tumors occurring in children to young adults, have genetic signatures implicating derivation from biliary tree stem cell (BTSC) subpopulations, co-hepato/pancreatic stem cells, involved in hepatic and pancreatic regeneration. FLCs and BTSCs express pluripotency genes, endodermal transcription factors, and stem cell surface, cytoplasmic and proliferation biomarkers.

The FLC-PDX model, FLC-TD-2010, is driven $ex\ vivo$ to express pancreatic acinar traits, hypothesized responsible for this model's propensity for enzymatic degradation of cultures. A stable $ex\ vivo$ model of FLC-TD-2010 was achieved using organoids in serum-free Kubota's Medium (KM) supplemented with 0.1% hyaluronans (KM/HA). Heparins (10 ng/ml) caused slow expansion of organoids with doubling times of \sim 7–9 days. Spheroids, organoids depleted of mesenchymal cells, survived indefinitely in KM/HA in a state of growth arrest for more than 2 months. Expansion was restored with FLCs co-cultured with mesenchymal cell precursors in a ratio of 3:7, implicating paracrine signaling. Signals identified included FGFs, VEGFs, EGFs, Wnts, and others, produced by associated stellate and endothelial cell precursors.

Fifty-three, unique heparan sulfate (HS) oligosaccharides were synthesized, assessed for formation of high affinity complexes with paracrine signals, and each complex screened for biological activity(ies) on organoids. Ten distinct HS-oligosaccharides, all 10–12 mers or larger, and in specific paracrine signal complexes elicited particular biological responses. Of note, complexes of paracrine signals and 3-O sulfated HS-oligosaccharides elicited slowed growth, and with Wnt3a, elicited growth arrest of organoids for months. If future efforts are used to prepare HS-oligosaccharides resistant to breakdown *in vivo*, then [paracrine signal—HS-oligosaccharide] complexes are potential therapeutic agents for clinical treatments of FLCs, an exciting prospect for a deadly disease.

Introduction

Fibrolamellar carcinomas (FLCs), deadly cancers affecting children to young adults were rare prior to World War II but have increased in occurrence since then, becoming a significant percentage of endodermal cancers [1,2]. The reason(s) for the recent increase in occurrence is unknown. FLCs were considered originally to be variants of hepatocellular carcinomas (HCCs) or cholangiocarcinomas (CCs), but recent genetic signature analyses have indicated their derivation from biliary tree stem cell subpopulations, co-hepato/pancreatic stem/progenitors, participating throughout life in hepatic and pancreatic regenerative processes [3,4].

Hepato/pancreatic stem cell subpopulations are present in all mammals evaluated and are located in the duodenal submucosal glands (dSGs), also called Brunner's Glands, and in peribiliary glands (PBGs) throughout the biliary tree [4-11]. These are referred to as duodenal submucosal gland (dSG) stem cells [5] and biliary tree stem cells (BTSCs) [4,6-8,11]. They are linked maturationally to late-stage stem cells in the gallbladder, that has no PBGs [11], and to the hepatic stem cells and hepatoblasts in or near the canals of Hering [12-15] and that are the precursors to hepatocytes and cholangiocytes within the liver acinus. In parallel, BTSCs are precursors also to pancreatic stem cells found in PBGs in the hepato-pancreatic common duct and linked maturationally to pancreatic ductal committed progenitors in pancreatic duct glands (PDGs) within the pancreas and from them to acinar cells and islets [9,16,17].

Previously, we established the first FLC-PDX model [3], that along with analyses on freshly isolated FLCs, has been used by a number of

investigators to explore FLC biological phenomena [18-24]. There are now additional PDX models established in the past year or so and enabling appreciation of generic patterns of phenomena in FLCs [25] such as their extremely slow growth in immunocompromised hosts and very slow *ex vivo* growth under known culture conditions. The slowness *in vivo* and *ex vivo* has obviated many types of experimental studies [3, 25]. This complication is further exasperated by FLCs' production and release of matrix-degrading enzymes, causing loss or instability of cultures.

Alternatives were attempted by inserting into established cell lines, both human ones and murine ones, the fusion gene unique to FLCs, an oncogene (DNAJB1–PRKACA) encoding a fusion protein (DNAJ–PKAC) in which the J-domain of a heat shock protein 40 (HSP40) co-chaperone replaces an amino-terminal segment of the catalytic subunit of the cyclic AMP-dependent protein kinase (PKA) [21,22,26]. Such cell lines with an inserted fusion gene were found to mimic only a subset of the key features of FLCs, implicating additional genetic variables associated with FLCs. Other variables, such as BAP mutations, have been found also relevant [27,28] . The most elegant of these investigations has been a study in which human fetal liver cells were transduced with specific genes or knockouts (KO) of specific genes were achieved [29]. It was found that cells with BAP1-KO and PRKAR2A-KO double mutants were able to yield traits relevant to FLCs and were able to grow in a medium designed for human ductal epithelial organoids.

The most successful *ex vivo* format for FLCs has proven to be organoid cultures, floating aggregates of FLCs in association with their mesenchymal precursor cell partners, precursors to endothelia and stellate cells [3,25]. Organoids were established from the original FLC-PDX model, FLC-TD-2010 [3] under conditions consisting of serum-free Kubota's Medium (KM), a wholly defined medium designed for endodermal stem cells, with a rich basal medium containing key trace elements (e.g. selenium and zinc), but not copper, low calcium (0.3 mM), and devoid of hormones and growth factors except for insulin, transferrin/Fe, high density lipoprotein (HDL) and a mixture of free fatty acids bound to purified albumin [30]; it was found to stabilize FLC organoids further if supplemented with 0.1% hyaluronans (referred to as KM/HA).

Hyaluronans (HA), non-sulfated polymers of the dimer, p-glucuronic acid (GlcA) and N-acetyl-p-glucosamine, and their receptors, such as CD44, are key components of stem cell niches [31,32] and were found in these studies to offer stabilizing effects on organoids of FLCs and of

Jian Liu, PhD. UNC School of Pharmacy 1044 Genetics Building, CB# 7356, Chapel Hill, NC 27599; Phone: 919–843–6511. Email: liuj@email.unc.edu. Senior corresponding author with respect to glycosaminoglycan chemistry and preparation of synthesized heparan sulfates

⁶ Zhiying He, PhD. Institute for Regenerative Medicine, Shanghai East Hospital, School of Life Sciences and Technology, Tongji University, Shanghai, China, 200123. Email: zyhe@tongi.edu.cn. Phone: +86-21-20334518-22241. Senior corresponding author with respect to bioinformatics and genetic signature studies

Jola M. Reid, PhD. 5200-G MBRB CB# 7038, UNC School of Medicine, Chapel Hill, NC 27599; Senior corresponding author with respect to endodermal stem cell biology, matrix chemistry and biology, and organoids

BTSCs. Here we present evidence that regulation of expansion versus differentiation of FLCs and of BTSCs is mediated by paracrine signals in complexes with glycosaminoglycans (GAGs), polymers of the dimers, glucuronic acid and an amino sugar [33,34] Figures S7 and S8. Two of the major families of the GAGs are:

- Chondroitin sulfates (CS), sulfated polymers of the dimers, N-acetylgalactosamine (GalNAc) and glucuronic acid (GlcA), and that include specific forms of CSs, identified as important matrix components in stem cell niches and critically involved in facets of development [35-38]. In recent studies [39], we found that CS biosynthesis genes, especially the rate-limiting enzyme, chondroitin sulfate's N-acetyl galactosamine transferase 1 (CSGALNACT1), and CS chains are increased dramatically in FLCs relative to their expression levels in normal hepatic organoids. In parallel, a key chondroitin sulfate proteoglycan (CS-PG), versican (VCAN), is highly expressed in FLCs, indeed at levels significantly greater than in other cancers [39]
- Heparan sulfates (HS) and heparins (HPs), sulfated polymers of the disaccharides of GlcA or IdoA and sulfated glucosamine, are present as side chains on heparan sulfate proteoglycans (HS-PGs) and heparin proteoglycans (HP-PGs) [40-42]. These chains bind tightly to proteins such as paracrine signals, influencing their three-dimensional conformation, their binding affinities to receptors, and dictating facets of signal transduction and cell functions [40,42-49]

GAGs participate in numerous biological processes, including embryonic development, influencing viral and bacterial infections, and regulating blood coagulation [40,50-52]. They are presented on the surface of cells in the forms of proteoglycans, which contain a core protein with GAG side chains [47,51,53-56]. Common cell surface proteoglycans on FLCs and BTSCs include syndecans, with core proteins that are transmembrane proteins, and glypicans that are bound to the plasma membrane by phosphotidyl inositol (PI) linkages [57-61]. Core proteins of proteoglycans can have activity on their own (e.g. the receptors for transferrin and colony stimulating factor), and there are considerable numbers of biological activities influenced by just the GAG chains [45,51,52,62]. Most commonly, these biological activities are due to the binding of soluble signals (growth factors, paracrine signals, cytokines, hormones) to specific GAG sequences, epitopes, in the chains and influencing biological responses directly or indirectly [40,48,51,52, 63]. The recent establishment using our strategies by which to synthesize structurally defined GAG chains makes possible investigations of the relevance of specific GAG chain chemistries to biological functions [42, 46,64,65].

Others have prepared organoids from new FLC-PDX models as well as the FLC-TD-2010 model under *ex vivo* conditions consisting of Matrigel and media richly supplemented with growth factors and hormones and sometimes also with serum supplementation [25]. The conditions are quite distinct from those used by us and that sustained the FLCs as stem cells. In this study we focused on mesenchymal cell precursors, derived from endothelia and stellate cells, that generate paracrine signals forming high affinity complexes with heparan sulfate (HS) oligosaccharides. These paracrine signal/HS complexes have been found to influence organoids of FLCs and their normal counterparts, BTSCs, in their expansion or differentiation.

The potency in this regulation of FLC organoids by some complexes of [paracrine signal and HS oligosaccharides] suggest that selected ones of them might offer therapeutic options for FLC patients. More detailed analyses of the effects of complexes of various [paracrine signals and synthesized HS oligosaccharides] with respect to organoids of normal human BTSCs and their maturational lineage derivatives, human hepatic stem cells, human hepatoblasts and adult human hepatocytes are to be provided in a future paper (Zhang et al. in preparation). In brief, the biological responses are dictated by the complexes of a specific

paracrine signal partnered with a specific synthesized oligosaccharide.

Results

Key conclusions regarding FLCs were generated in past studies [3, 18-20,24,66] and have been confirmed in the findings from new experiments as summarized below in a series of conclusions (A) (the data for these are presented in the online supplement) and serve as background for the new studies.

A.1. Conclusion: FLCs are genetically related to biliary tree stem cell (BTSC) subpopulations, and not to mature hepatic or pancreatic cells (Figure S1)

To identify FLCs in solid tumors, histological staining was done on paraffin sections of tumors from FLC xenografts in immunocompromised hosts, NSG mice. FLCs in these tumors were separated from the surrounding tissue by strong desmoplastic responses with bands of collagenous fibers detected with hematoxylin & eosin staining (H&E) (Figure S1.A).

Kubota's Medium (KM), a wholly defined medium established previously for *ex vivo* maintenance of hepatoblasts [30,67], has been found to work well for other endodermal stem cell subpopulations, including biliary tree stem cells, BTSCs and hepatic stem cells [3,7,12,30] and for organoids of both FLCs and BTSCs, floating cell aggregates partnered with early lineage stage mesenchymal cell precursors (ELSMCs), angioblasts and precursors of endothelia and of stellate cells [3] (Figure S1. B-F).

FLC cultures, both monolayer colonies and organoids, were associated with a wealth of exosomes, ones found to merge with neighboring mesenchymal cells (Fig. 1C). By supplementing KM with 0.1% hyaluronans (soluble; size = $\sim\!1.5\!-\!1.8\times10^6$ Da), resulted in more stable organoids. The conditions are referred to as KM/HA. FLCs maintained in KM/HA demonstrated slow but steady proliferative capacity with cell doublings every $\sim\!7\!-\!9$ days for 2 months or longer and were stable throughout with respect to their phenotypic traits.

FLCs were characterized using immunohistochemistry and RNA-seq analyses (Figure S1). The analyses revealed that expression levels of EpCAM and SOX17 were low in FLCs, and expression of PDX1, a marker of pancreatic precursors is high (Figure S1.H).

A.2. Conclusion: FLCs are rich in Cancer Stem Cells regulated by Oncogenic PKA Signaling.

Prior studies [3,19,20,68] plus current findings (Figure S1.H) demonstrated genetic signatures of early endodermal stem cells such as strong expression of endodermal transcription factors (e.g. OCT4, FoxA2, Nanog, KLF4, SOX9, SALL4, BMI1), and stem cell surface markers [e.g. sodium iodide symporter (NIS), multiple forms of CD44, both CD44s and CD44variants, LGR5] coupled with negligible, if any, expression of mature hepatic or pancreatic markers.

Recognition of FLCs as being rich in cancer stem cells was established previously [3,68]. The percent cancer stem cells in liver tumors has long been known to be, on average, a few percent in hepatocellular carcinomas (HCCs) and up to $\sim 10{\text -}12\%$ in cholangiocarcinomas (CCs) [69-72]. By contrast, FLCs are unique in being especially endowed with cancer stem cells [3,24,68]. In studies in which definitive tests, tumor initiating assays, were done on the FLC-TD-2010 PDX model, it was found particularly remarkable in being more than 70% cancer stem cells [3]. It is unknown if the newer FLC PDX models are similar, since they have not yet been subjected to such an assay [25].

The studies here complemented the prior findings resulting in recognition of other stem cell traits including aldehyde dehydrogenases (ALDHs) in organoids of FLC versus their normal counterparts, BTSCs (Figure S1.I-J). High ALDH activity is a classic feature of stem cells. When adding Aldefluor (Bodipy493/503-aminoacetaldehyde) and

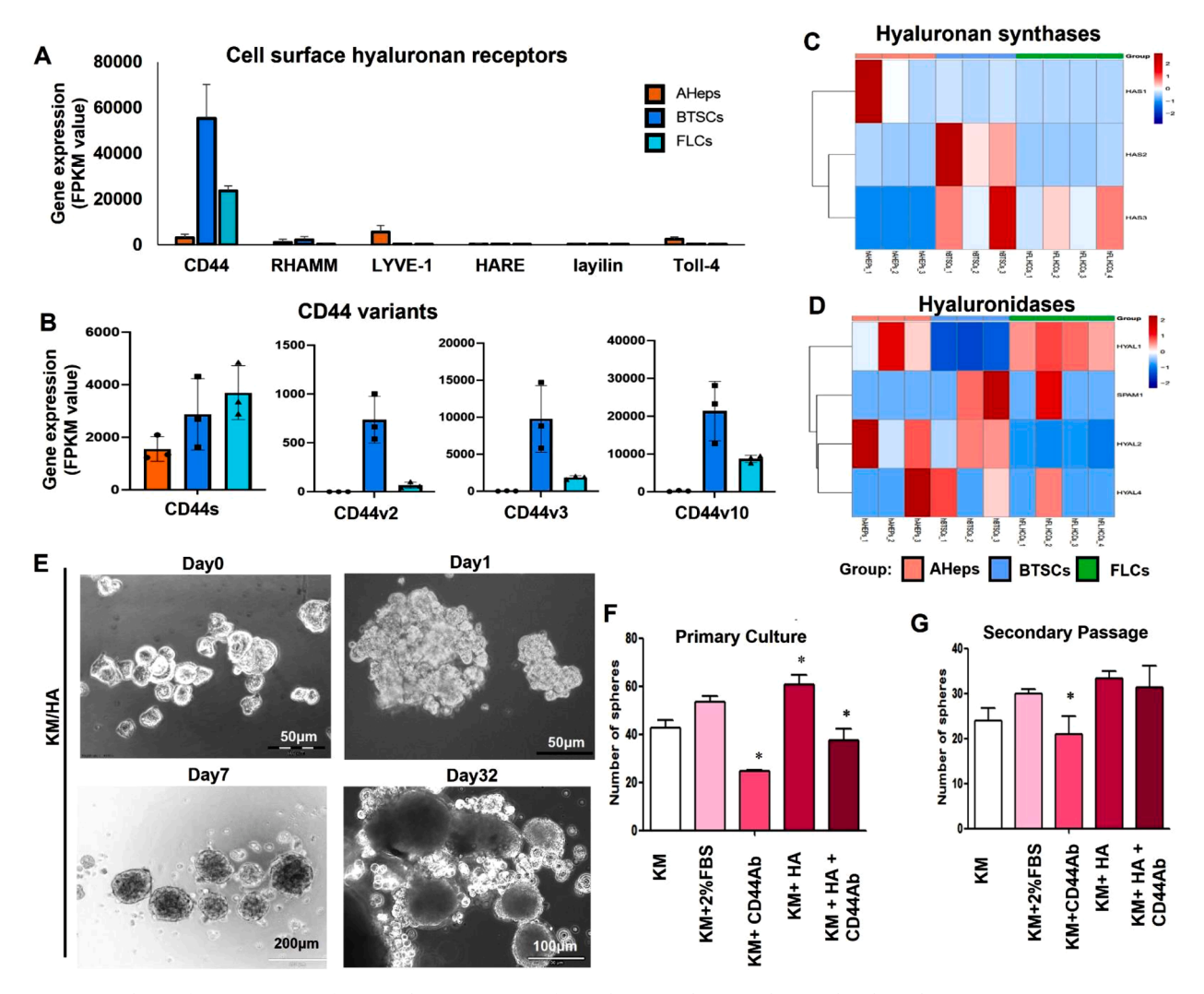


Fig. 1. Primary Conditions for Maintenance of Organoids *Ex Vivo*: Serum-free Kubota's Medium supplemented with Hyaluronans. Organoid cultures of FLCs (also the spheroids) were maintained in serum-free Kubota's Medium + 0.1% hyaluronans, referred to as KM/HA and were stable for at least several months.

A. Cell surface hyaluronan receptors include CD44, RHAMM, LYVE-1, HARE, laylin and Toll-1 were detected by RNA-seq of their expression patterns for adult hepatocytes (AHeps), BTSCs, and FLCs. CD44 was found as the major hyaluronan receptor for FLCs and BTSCs.

B. Different variants of CD44 include CD44v2-v10(CD44v2), CD44v3-v10(CD44v3) which has heparan sulfate moieties, and CD44v10 were investigated. CD44s and CD44v3, CD44v10 were found expressed in FLCs.

- C. Hyaluronan synthases, HAS1-3 were found expressed in FLCs. HAS3 was significantly expressed in FLCs and BTSCs, but was low in adult hepatocytes.
- D. Hyaluronidases, especially HYAL1, was found expressed in FLCs.
- E. Morphologies of FLC organoids in Kubota's Medium + 0.1% hyaluronans in day 0, day 1, day 7 and day 32.
- F. Effects of HA and FBS were detected by adding HA and CD44 antibody and 2% FBS in the KM during the culture of FLC spheroids. *p<0.05:
- G. Effects of HA and CD44 antibodies on the second passage (P2) organoids after enzymatic digestion.

AldeRed™ 588-A (or Bodipy576/589-aminoacetaldehyde) to the culture medium of BTSC organoids versus FLC organoids, both showed the capability of converting an ALDH substrate, which diffuses into the cells of organoids and produces green or red fluorescence (Figure S2). However, the proportion of green and red signaling were distinct in BTSC organoids versus FLC organoids. All cells in the BTSC organoids were Aldefluor⁺, and only the cells at the surface of the BTSC organoids were AldeRed⁺. While all the FLC organoids were AldeRed⁺, with only a portion of them being Aldefluor⁺. This distinct pattern of responding to the two ALDHs reagent was complemented by the ALDH gene expression analyses; the expression patterns of the 20 ALDH members in FLCs, BTSCs, and adult hepatocytes (AHeps) indicated that the major types of ALDH in FLCs are ALDH1A and ALDH2 and to less extent, ALDH3B1; by contrast, those in BTSCs are ALDH1A3. An ALDH inhibitor, diethylaminobenzaldehyde (DEAB), was used in the negative control group for the background fluorescence assessment. Although the findings

support the realization of FLCs and BTSCs as being stem cell subpopulations, it is not known what the relevance is of the different proportions and the different types of ALDH in the BTSCs versus FLCs.

A recent report from the collaborative efforts of several groups of investigators have used a cell line, FLX1, established from the FLC-TD-2010 PDX model by Bardeesy and associates, and have shown that it has oncogenic aberrations in PKA in a signaling network channeling through Myc oncoproteins [73].

A.3. Expansion of conclusion that FLCs are notoriously difficult to maintain *ex vivo* because of expression of degradative enzymes.

FLCs from FLC-TD-2010 have a propensity for autolysis and destruction of culture environments due to production of pancreatic acinar enzymes and matrix metalloproteinases (MMPs) (Figure S3). This

FLC-PDX model preserved the histological structure of FLCs when transplanted subcutaneously in NSG mice, but when under various *ex vivo* conditions, they resulted in destruction of the cultures. These FLC cultures rapidly (within hours) lost attachment to culture dishes, even ones coated with purified matrix components and even when plated onto a substratum of a liver-specific biomatrix scaffold extract and in KM [74,75]. Remarkably, the FLCs caused complete dissolution of the matrix substrata and even of the biomatrix scaffold within less than 24 h. Under these conditions, the FLCs were found to express genes encoding exocrine enzymatic activity, such as trypsinogens, serine protease 3 (PRSS3), and carboxypeptidase D, E and M (CPD, CPE, CPM) (Figure S3, C, Table S1). The overall expression level of matrix metalloproteinases (MMPs), especially MMP17, MMP26, and MMP27, were significantly higher in FLCs compared to levels in normal liver tissues or in BTSCs (Figure S3).

Carboxypeptidase (CPE), a member of the family of carboxypeptidases, is highly expressed by both primary and metastatic FLC tumors but not by non-malignant liver tissues. A trypsinogen, serine protease inhibitor Kazal-type I (SPINKI), which is also a marker for functional pancreatic exocrine cells, was found to be expressed only in metastatic FLC tumors but not in primary tumors nor by non-malignant tissues.

A.4. Conclusion: attempts at differentiation *ex vivo* yielded stable effects in BTSCs but only transient ones for FLCs

Additional *ex vivo* studies demonstrated further the rich stemness traits of these FLCs in their response to hormonally defined media, HDM, used to drive expansion versus differentiation of cells under serum-free, wholly defined conditions [3,74]. Similarly to that found previously [3], the organoids of BTSCs, but not those of FLCs, were able to differentiate towards adult fates if subjected to an HDM for differentiation towards an hepatocyte fate (HDM-H), a cholangiocyte fate (HDM-C) or a pancreatic islet cell fate (HDM-P). The differentiation of the BTSCs correlated with the loss of expression of stem cell traits (e.g. LGR5, CD44 and pluripotency genes) and acquisition of expression of genes that are part of the genetic signature indicative of one of the adult fates. Although FLC organoids did respond to the distinctive HDM, the responses were transient, lasting only hours to less than a day and then reverting to the genetic signature that was rich in stem cell traits and similar to that of FLC organoids maintained in KM/HA [3].

Key signaling within organoids

With the above as background, we focused on learning what regulates growth versus differentiation of FLCs in comparison to their normal counterparts, BTSCs. This was done using organoids of FLCs or BTSCs partnered with early lineage stage mesenchymal cells (ELSMCs), comprised of angioblasts [CD117 $^+$ or CD133 $^+$, co-expressing vascular endothelial growth factor receptor (VEGFR2) and kinase insert receptor (KDR)] and precursors to endothelia [CD31 $^{++}$ and KDR $^+$] and to stellate cells [CD146 $^+$, ICAM-1 $^+$, vascular cell adhesion molecule (VCAM-1)] as shown previously [3,7,67,74,76,77].

Conditions for stable organoid cultures (Fig. 1)

FLC organoid cultures in KM/HA were stable sufficiently for long-term cultures of weeks to months. As shown, hyaluronan cell surface receptors, CD44 and multiple CD44 isoforms, were found to be expressed by FLCs and their normal counterparts, BTSCs. We detected expression of other hyaluronan receptors (RHAMM, LYVE-1, HARE, layilin and Toll-4) in FLCs, but the isoforms of CD44 proved the most expressed hyaluronan receptors in FLCs (Fig. 1A). FLCs showed expression of CD44s plus CD44v2-v10 (CD44v2) and CD44v3-v10 (CD44v3, known to bind to heparan sulfates, enabling joint effects of hyaluronans and heparan sulfates on the cells in cultures (Fig. 1B).

The RNA-seq analyses were used also to evaluate hyaluronan

synthases (HASs, Fig. 1C) and hyaluronidases (HYALs, Fig. 1D). The studies on three hyaluronan synthases (HAS1, HAS2, HAS3), analyzed in FLCs, BTSCs and adult human hepatocytes (AHeps), revealed that HAS3 was under expressed in other tumor types but highly expressed in FLCs and BTSCs. The expression of HAS3 is commonly related to expansion of the cell surface hyaluronan coat, which inhibits the sensitivity of FLCs to proliferation factors in cultures. Interestingly, the hyaluronidase, especially HYAL1, commonly found to increase tumor cell proliferation, is also expressed by FLCs (HAS3 and HYAL1 in FLCs maintained in KM/HA) suggesting an association with mild proliferative responses (Fig. 1D).

When adding 0.1% HA into KM (KM/HA), FLC cells formed aggregates within 12 h, and continued to form organoids with diameters of $\sim\!100\!-\!200\,\mu m$ by 7 days. The FLC organoids could be maintained under the KM/HA condition long-term as shown in Fig. 1E. Adding an antibody targeting CD44 during the formation of FLC organoids resulted in a significant reduction in the number of organoids formed (Fig. 1F). Adding HA back to the KM in combination with the antibodies partially restored the number of organoids (Fig. 1G). However, this effect of HA on the CD44-antibody-treated organoids was lost by the second passage of the organoids after enzymatic dissociation. Evaluation of the effects of hyaluronans on cell proliferation indicated that they increased stability of the organoids, and had a minor effect on the number of organoids generated in the first passage, but an effect that did not persist with passaging.

Spheroids versus organoids: paracrine signaling is essential for FLC biological responses (Fig. 2)

FLC tumors from FLC-TD-2010 transplantable tumors in NSG mice were enzymatically dispersed and subjected to FACS sorting to deplete the mesenchymal precursor cells. Approximately $50{\sim}70\%$ of the cell mixture of the digested FLC-TD-2010 tumor proved to be mouse mesenchymal cells, which could be recognized by an H2K^d antibody, findings established in a previous study[38] (Figs. 2A, B). This resulted in FLC spheroids, floating aggregates of FLCs with minimal levels of their mesenchymal cell partners (Figs. 2C-D). The FLC spheroids survived for months $ex\ vivo$ in KM/HA but with negligible growth. The doubling times of the spheroids were approximately a division every ${\sim}60{-}70$ days (Fig. 2E). This indicated a need for paracrine signals derived from the interactions of FLCs with mesenchymal precursor cells for the growth of the FLCs.

To confirm the requirement for paracrine signaling from mesenchymal cell precursors for FLC proliferation, we co-cultured FLC spheroids with human fetal tissue-derived mesenchymal cells in ratios of 1:9 and up to 9:1 during the passaging (Fig. 2F). We found when digesting cultures of freshly isolated FLCs from transplantable tumors (xenografts in NSG mice) for 15 min with 0.25% trypsin, mesenchymal precursor cells were killed. Remaining FLC cells lost their ability to proliferate and went into growth arrest lasting for over 8 weeks. However, when co-culturing FLC spheroids with freshly isolated fetal human mesenchymal cells at a ratio of 7:3, the FLC were able to achieve a proliferation rate comparable to that in the organoids of approximately a division every 7–9 days. The co-cultures elicited distinctive changes in the morphology of FLCs and along with the effects on proliferation indicated that paracrine signaling from mesenchymal cell precursors is critical for FLCs, especially for cell division (Fig. 2C-E).

Paracrine signals identified (Figs. 3-5)

The genetic signatures of FLCs and BTSCs versus AHeps revealed key paracrine signals. The ones with peak expression were vascular endothelial growth factor (VEGF), particularly VEGFA-; fibroblast growth factors (FGF), particularly FGF2 and its receptors, FGFRs; and especially Wnt7B and its receptor, Frizzle 10. Of the many forms of FGFs, the most highly expressed in FLCs were FGF2 and its receptor FGFR1. VEGFA in

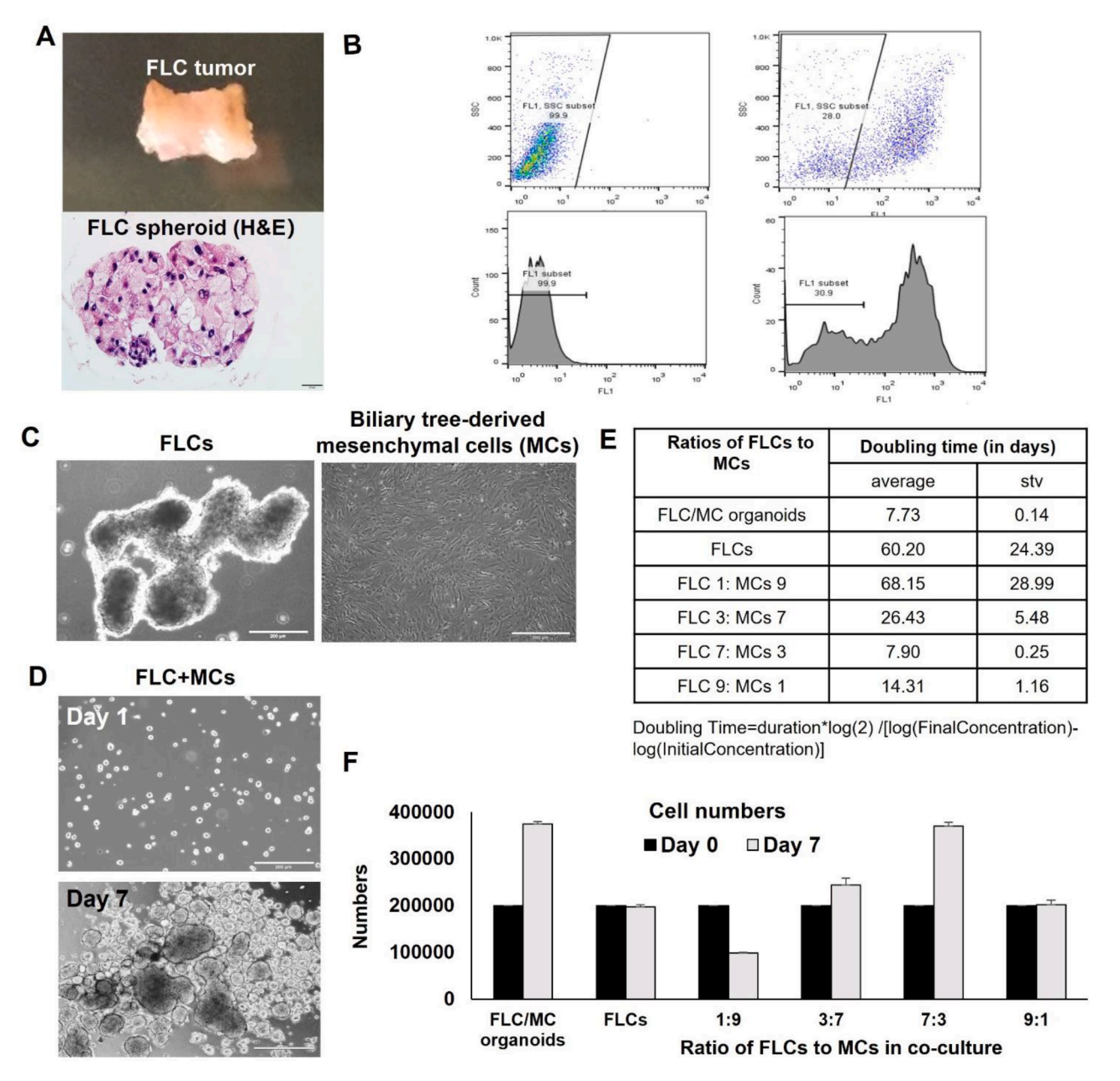


Fig. 2. Spheroids vs Organoids—Paracrine Signals Critical for many Biological Responses.

Organoids, floating aggregates of FLCs and mesenchymal cell precursors comprising precursors for stellate cells and endothelial cells. Spheroids are floating aggregates of FLCs from which the mesenchymal cells have been depleted by magnetic bead immunoselection.

- A. FLC tumor and H&E-stained section of a FLC spheroid.
- B. Flow cytometric analyses for the percentage of mesenchymal cells versus human FLCs in cell suspensions prepared from the transplantable tumor line, FLC-TD-2010.
- C. Morphologies of FLC organoids (C-left) and biliary tree-derived, early-stage mesenchymal cells (MCs, C-right) maintained in serum-free Kubota's Medium supplemented with 0.1% hyaluronans.
- D. Original passage of FLC organoids was trypsinized to obtain cell suspensions and then was subjected to magnetic bead immunoselection to remove the murine mesenchymal cells. Selection was achieved with a cocktail of biotin-conjugated anti-mouse antibody against lineage cells (1:10 dilution, Miltenyi Biotech) and with biotin-conjugated anti-mouse-MHC class I (H2Kd, clone SF1–1.1, 1:100 dilution). Morphology of re-formed FLC organoids when mixed with mesenchymal cells from C-right in various ratios. Shown are organoids of FLCs partnered with mesenchymal cells at a ratio of 7:3.
- E. Doubling time for reconstituted FLC organoids generated from mixing of FLC with mesenchymal cells. Passage 0 organoids were digested with trypsin to obtain single cell suspensions and then the FLC: MC ratios were varied. The FLC: MC ratios assessed were 1:9, 2:8, 3:7, 4:6, 5:5, 6:4, 7:3, 8:2, 9:1. The controls were 20, 000 MCs or 20,000 FLCs in every well of the 6-well-low attachment-plates. Spheroids, aggregates of highly enriched FLCs and with minimal numbers of mesenchymal cells, divided very slowly, about once after 61 days. The organoids, especially those with a ratio of FLC:MC of 7:3 divided the fastest and underwent a division every ~7 days.
- F. Histograms for showing the cell numbers of reconstituted FLC organoids. The ones with the most rapid cell division were those with a ratio of 7:3 of FLC: MCs.

FLCs was at a similar level as that in BTSCs and in AHeps, but VEGFR-1 is poorly expressed in FLCs. We were able to analyze directly the effects of FGF2 and VEGFA.

The most important of the Wnt ligands, Wnt7b, is expressed highly in FLCs along with the frizzle receptor (Fig. 3D). By contrast Wnt3A is not expressed significantly (Fig. 3E), though we found significant biological responses for it as demonstrated later in the findings presented in Figs. 8-10.

Interestingly, many of the paracrine signals such as epithelial growth factor (EGF) and R-spondin (RSPO1), were poorly expressed in FLCs, whereas their receptors were highly expressed. This included the EGF-receptor (EGFR), the leucine-rich-repeat-containing G-protein-coupled receptor 5 (LGR5), the receptor for R-Spondin, and the MET receptor, all

significantly expressed by FLCs (Fig. 3E and 3F).

To identify which cell types in the organoids of the FLC tumors generate the paracrine signals required for the proliferation of FLC cells, we did bioinformatic analyses (Figs. 4-6) of the dataset of snATAC-seq on non-malignant liver (NML) versus for primary and metastatic FLC tumors generated in previous studies [78]. By using the ArchR pipeline [79] to show markers identified in our previous study with the FLC-PDX model [3], we assigned each cluster to a specific cell type, including immune cells (PTPRC, CD3E, CD79A, CD68, C1QA, C1QB); endothelia (PECAM1, VWF, CD34); fibroblasts or stroma (ACTA2, DCN, LUM, FGF7, PDGFRB); hepatocytes (APOC3, FABP1, APOA1, FAH, ALB); cholangiocytes (TM4SF4, ANXA4, KRT7, CFTR, AQP1, AQP4, SLC4A2, SLC4A4); and FLC tumor cells (PDX1, TOP2A, ALDH1A1, VCAN, BMI1,

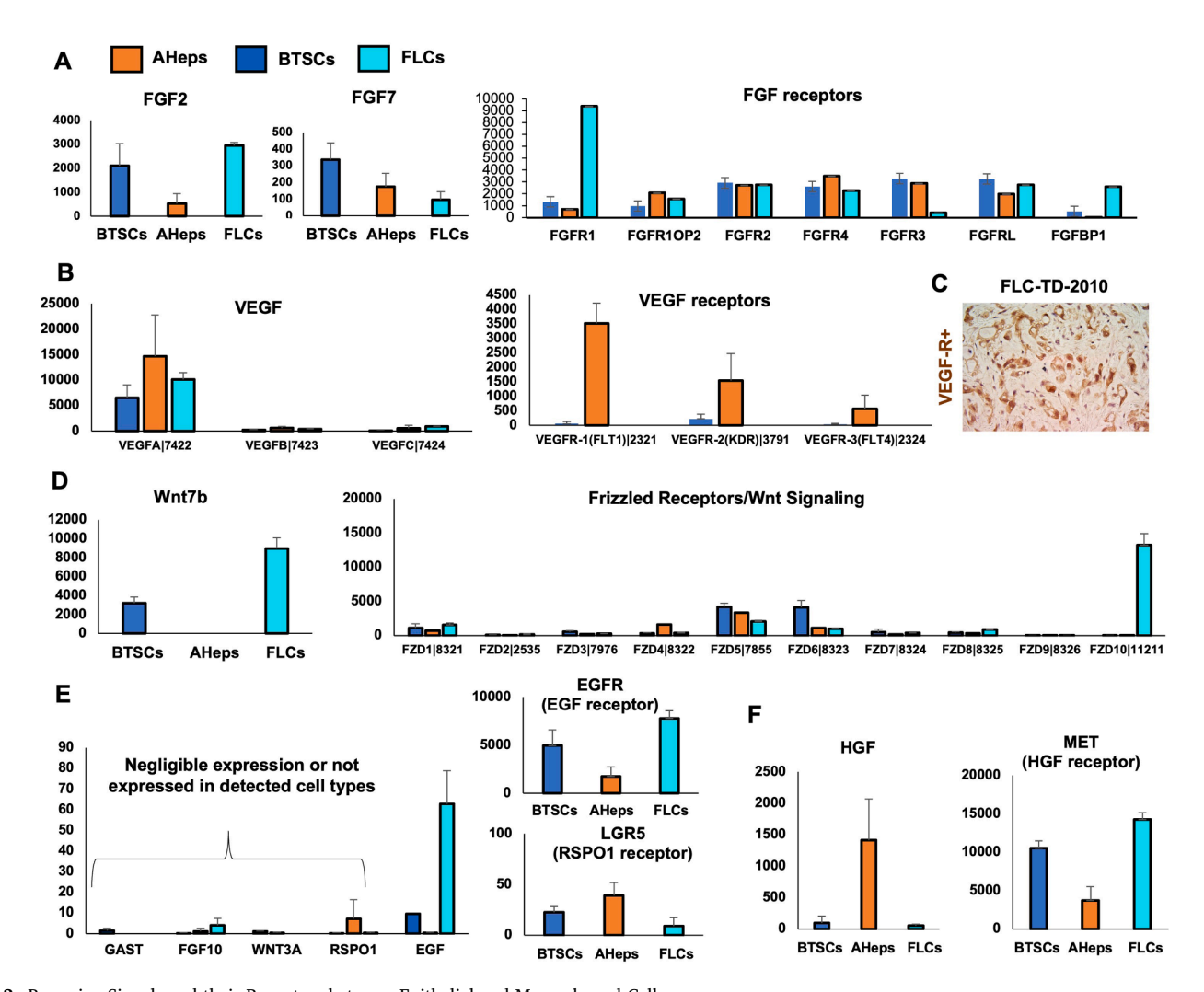


Fig. 3. Paracrine Signals and their Receptors between Epithelial and Mesenchymal Cells.

A. RNA-seq data of expression patterns of the fibroblast growth factor family (FGFs) and the FGF receptors (FGFRs) for human biliary tree stem cells (BTSCs, dark blue bar), adult human hepatocytes (AHeps, orange bar) and fibrolamellar hepatocellular carcinoma (FLC, light blue bar). Here FLC is represented by organoids. FGF7 is commonly added to the organoids formation system used for obtaining mature liver organoids from normal liver or from tumor tissue.

- B. RNA-seq data of expression patterns of vascular endothelial growth factor family (VEGFs) and VEGF receptors (VEGFRs) for BTSCs, AHeps, and FLC organoids. C. Immunohistochemistry staining of VEGFR1 of primary FLC tumor. The brownish red staining in the image indicates the positive expression of VEGFR1 in the FLC tumor cells. No counterstain was applied for this assay.
- D. RNA-seq data of expression patterns of most of the Wnt receptor and its receptors, the Frizzled families for BTSCs, AHEPsAHeps, and FLC organoids. This is to be compared to the highest expression, that for Wnt7b. Note: we were not able to test Wnt7b, since it is not available.
- E. RNA-seq data of expression patterns of other growth factors used in the liver organoids and cholangiocyte organoids formation system (that used in the work of others) for expanding the FLC cells from the primary cell mixture isolated from the tumor [25]. Expression of growth factors including Gastrin (GAST), FGF10, Wnt3a and R-spondin1(RSPO1) were negligible or not detected at all in BTSCs, AHeps, and FLC organoids. While epidermal growth factor (EGF) was found to be expressed in FLC organoids but not in AHeps. The expression patterns of EGF receptor (EGFR), and Leucine-rich repeat containing G protein-coupled receptor (LGR5), the receptor of R-spondin 1 were also compared in BTSCs, AHeps, and FLC organoids.
- F. RNA-seq data of expression patterns of hepatocyte growth factor (HGF) and its receptor mesenchymal epithelial transition (MET) for BTSCs, AHeps, and FLC organoids.

SLC5A5, SHH). We detected robust enrichment of growth factors and their receptors in FLC tumor cells versus other cell types. The findings are similar to those revealed by the RNA-seq data in Fig. 3. FLC tumor cells expressed VEGFA, GAST, EGF, EGFR, MET and FGFR4. In contrast, the expression of FGF2 and Wnt3a were not detected or in a low genome accessibility state in all cell types detected.

These analyses of the sources of the paracrine signals indicated that they are produced in part by FLCs and in part by stellate cell and endothelial cell precursors that are closely associated with the FLCs in the organoids, with the FLCs expressing enrichment for receptors for the signals.

Heparan sulfate biosynthesis, heparan sulfate proteoglycans, and heparanase (Fig. 7)

Heparan sulfate proteoglycans (HS-PGs) have long been known critical for regulation of coagulation [80-82], and their heparan sulfate (HS) chains known to form complexes with myriad proteins, including

those involved in coagulation and in paracrine signaling [49,83-85]. In so doing, HS-PGs and HSs influence many aspects of signal transduction particularly with respect to paracrine signals, such as FGFs, HGFs, VEGFs, EGFs, and Wnt ligands [86-88]. To clarify their roles in FLCs and BTSCs, we assessed the expression patterns of HS-PGs and found them to be expressed at normal levels relative to levels found in BTSCs. Of these, syndecan 1 and 4 and glypican 1 were expressed at significant levels in FLCs; BTSCs expressed these and also expressed glypican 4 (Fig. 7A). The results for heparan sulfates and for HS-PG were found at significant but reasonably normal levels in FLCs versus BTSCs.

This is in striking contrast to the findings for chondroitin sulfates (CSs) and chondroitin sulfate proteoglycans (CS-PGs), found at dramatically elevated levels in FLCs. This is especially true for Versican, a CS-PG found to be more than 8-fold higher in FLCs relative to its levels in normal cells [39].

Similar to the internal balance of HAS3 and HYAL1 in FLCs, we also detected gene expression levels of heparanase (HPSE) in FLCs, and that were compared to those of hepatocellular carcinomas (HCCs),

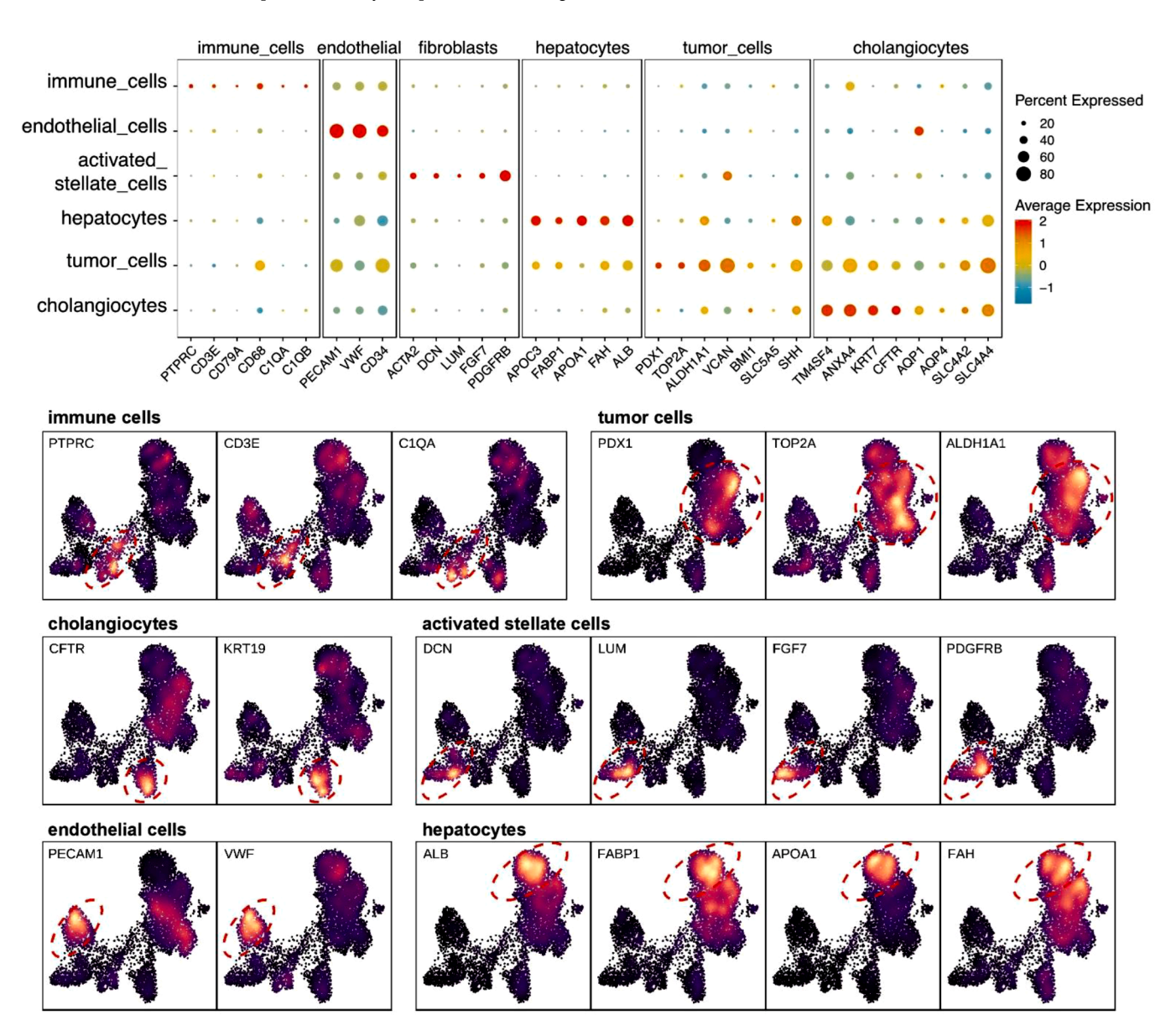


Fig. 4. Identification of Cell Types from snATAC-seq Data with defined markers.

FLC markers identified in previous study were used for clustering cells into six categories of cell types: immune cells (PTPRC, CD3E, CD79A, CD68, C1QA, C1QB); endothelia (PECAM1, VWF, CD34); fibroblasts or stroma (ACTA2, DCN, LUM, FGF7, PDGFRB); hepatocytes (APOC3, FABP1, APOA1, FAH, ALB), cholangiocytes (TM4SF4, ANXA4, KRT7, CFTR, AQP1, AQP4, SLC4A2, SLC4A4); and FLC tumor cells (PDX1, TOP2A, ALDH1A1, VCAN, BMI1, SLC5A5, SHH).

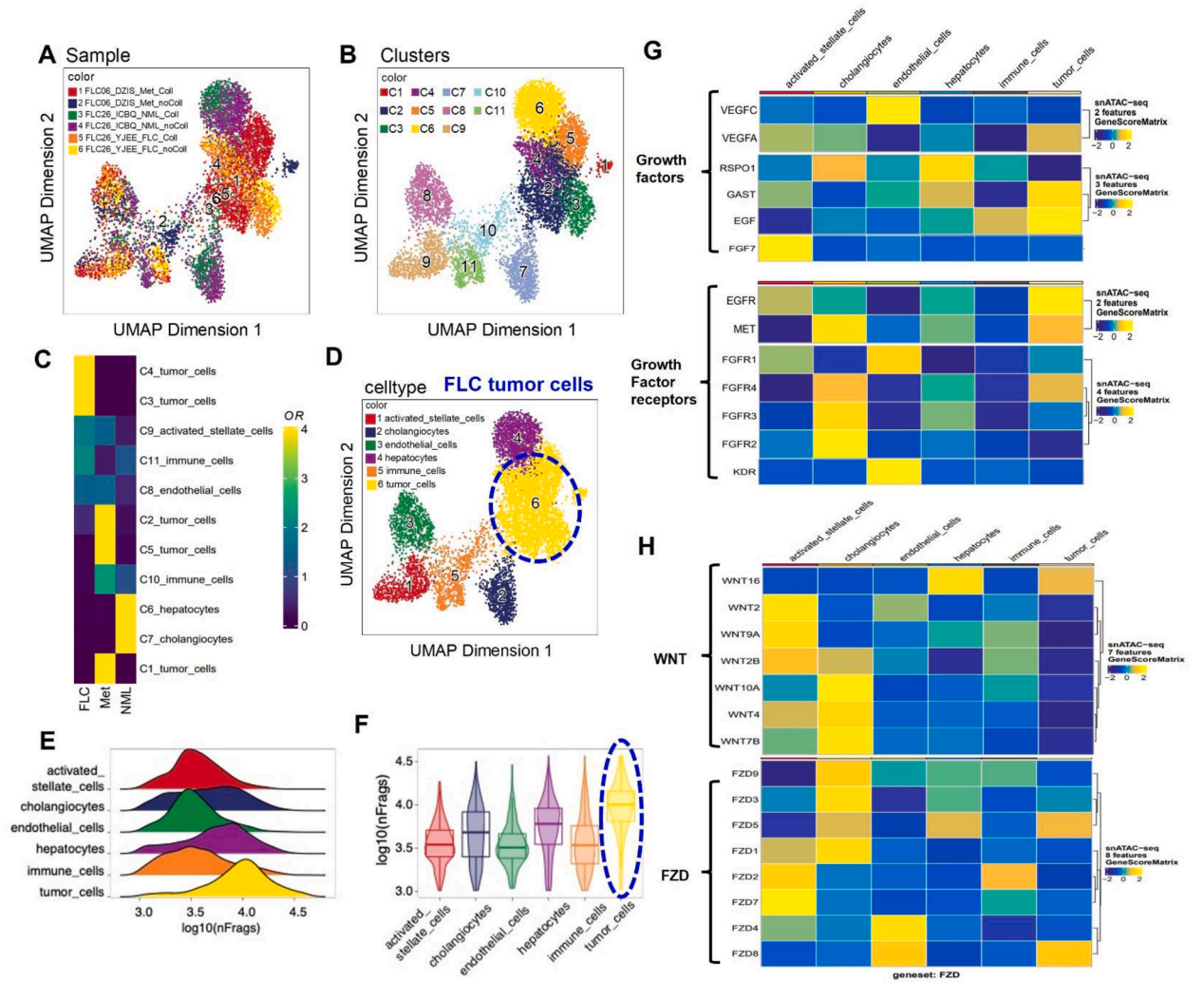


Fig. 5. Single-nucleus ATAC-seq Reveals Origins of Paracrine Signals for FLCs.

A-B. UMAPs of snATAC-seq from FLC tumor and nonmalignant liver tissues with or without collagen treatment, colored by aligned clusters.

C. Indexes characterizing meta-clusters and STARTRAC analysis were used to characterize the tissue distribution of meta-clusters; odds ratios (OR) were calculated and used to indicate preferences. In total, six clusters were indicated as tumor cells.

D. In total, 6 clusters of cell types were assigned for further analysis.1: activated stellate cells; 2: cholangiocytes; 3: endothelial cells; 4: hepatocytes; 5: immune cells; and 6: tumor cells (FLCs)

E-F. The overall activation of gene expression in the six clusters.

G-H. Expression patterns of Wnt and Wnt receptors, FGF and FGFR, VEGF and VEGFR, HGF and Met, RSPO1 and LGR5, EGF HGF and EGFR in the six clusters. Each plot focuses on one gene and the cell type in which it is more robustly active (black is low; yellow is high). Each dot in the plot corresponds to a particular cell and each clump of cells corresponds to a different cell type. The gene score was calculated using the ArchR package.

cholangiocarcinomas (CCs), and normal liver. There was no significant difference in the levels among the types of tumors and that in normal liver tissues (Fig. 7B). However, when using RNA-Seq to compare HPSE expression for AHeps versus BTSCs and FLC organoids, FLCs had significantly lower expression of HPSE compared to that in BTSCs and AHeps (Fig. 7C).

Further analyses of non-parenchymal cells in the tumors included recognition of stellate cells (CD146⁺), endothelia (CD31⁺), and hematopoietic precursors (CD45⁺). These 3 categories of non-parenchymal cells plus hepatocytes and BTSCs have significantly higher levels of expression of heparanase compared to the lower levels of expression in FLCs. This suggests that the presence of heparanase from precursors to stellate cells and endothelia in organoids in KM/HA may be a factor in regulation of proliferation of FLCs, an hypothesis yet to be tested (Fig. 7D).

HSs are key glycosaminoglycans (GAGs) responsible for binding to various proteins, such as paracrine signals [49,89]. They are linear

polysaccharides consisting of repeating units of N-acetylglucosamine (GlcNAc) and hexuronic acid (HexA) carrying sulfate groups in different backbones which can be synthesized and modified by a set of biochemical enzymes [65]. Sulfation is a dynamic and complex post-translational modification process [90]. It can occur at various positions within the GAG backbone and modulates different biological functions through effects on the 3-dimensional structure of the protein or its receptor [51,90].

When adding intestinal mucosa-derived heparin extracts, comprising a mixture of many HS-oligosaccharides of various length and sulfation patterns, to the serum-free Kubota's medium, the FLCs exhibited slow but significant growth within 7 days of culture (Fig. 7E). However, the screening of the synthesized heparan sulfate oligosaccharides did not result in the identification of one(s) that mimicked this response in FLCs.

The bioinformatic analyses of HS biosynthetic enzymes (Fig. 7F) indicated that the enzymes related to the elongation of HS chains, including exostosin 1 (EXT-1), glucuronic acid epimerase (GLCE), and

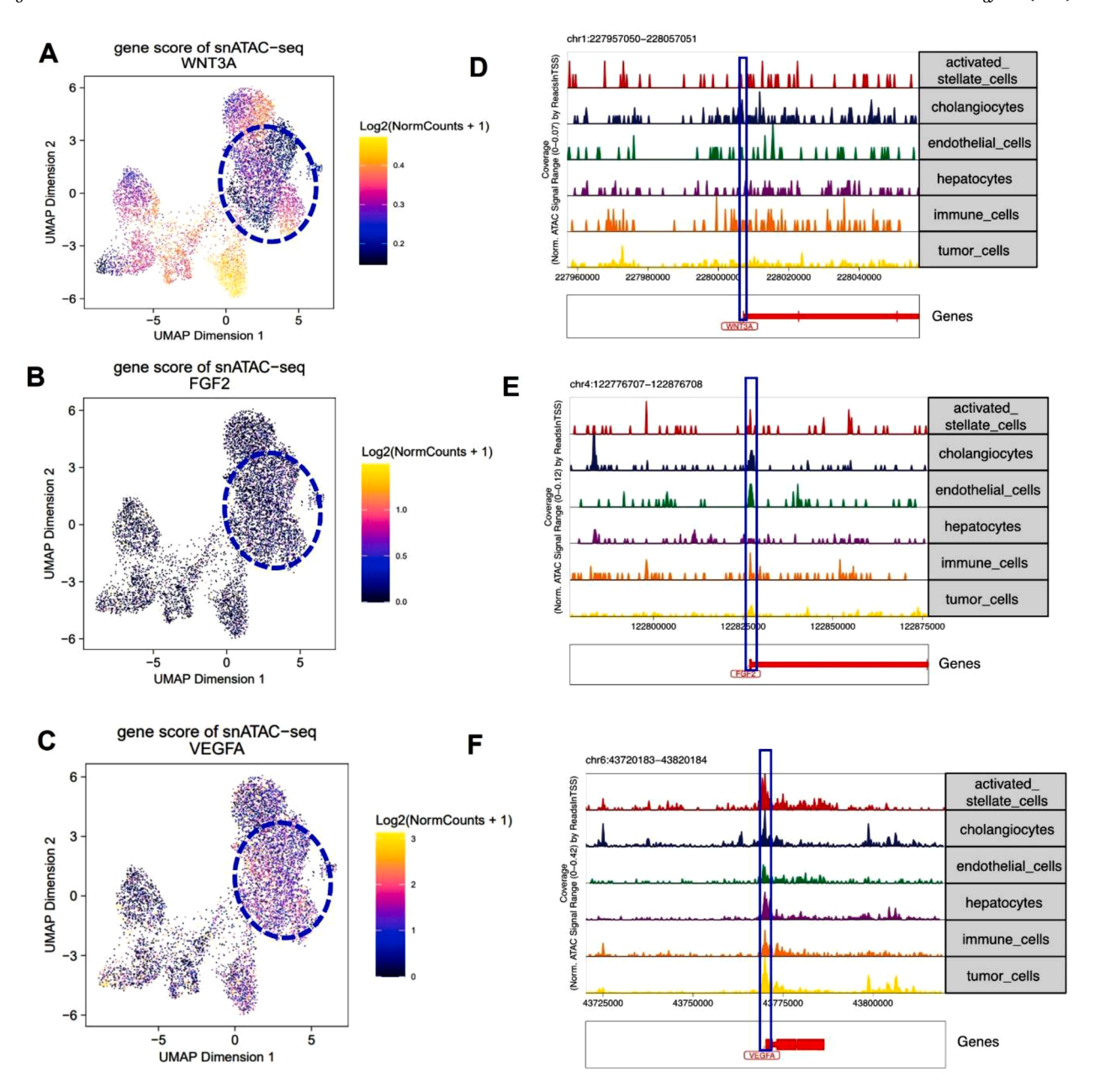


Fig. 6. Genome accessibility track visualization of genes encoding studied growth factors with peak co-accessibility. Single-nucleus gene expression score (exp.) of Wnt 3a (A), FGF2 (B), VEGFA (C) in the six cell types, as well as the genome track visualization of the Wnt3a locus (chr1:227,957,050–228,057,051) (D) and the FGF2 locus (chr8, 11,301,521–11,451,521) (E), and VEGFA locus(chr6:43,720,183–4,382,018) (F) in each cell type. The annotated transcriptional start site for Wnt3a, FGF2, and VEGFA are shown at the bottom of the panel, respectively.

PAPSS2 were highly expressed by FLCs compared to AHeps and BTSCs. Interestingly, a 3-O-sulfotransferase gene, HS3ST6, but not other enzymes, was also highly expressed in FLCs, which might explain the biological effects of 3-O-sulated HS-oligosaccharides on the FLCs.

In summary, FLCs expressed hyaluronans, hyaluronan receptors (CD44s, CD44v2, and CD44v3), two HS-PGs (syndecan 4 and glypican 1), and enzymes (hyaluronidase, MMPs and heparanase) involved in degradation of the matrix components required for internalization of endosomes with GAG/signal complexes.

HS-oligosaccharides and paracrine signals caused changes in the size of nuclei of biologically responsive cells (Fig. 8)

Early in the studies we learned that complexes of [paracrine signals and HS-oligosaccharides] were able to elicit biological responses that

were predicted reliably if they could elicit an increase in the size of the nuclei by 17–18 h of treatment of the cultures (Fig. 8A). The extent of the increase was significant (Fig. 8B). This became a routine assay in the screening of the [paracrine signal/HA-oligosaccharide] complexes to assess whether further biological studies were required.

HS-oligosaccharides forming high affinity complexes with paracrine signals (Fig. 9, Table S2)

By using a chemoenzymatic synthesis protocol [42,46], we obtained 53 HS-oligosaccharides with chain lengths varying from 5-mers to 18-mers (Figure S7 and S8). Consistent and reproducible biological effects were observed with HS chains that were 10–12-mers or larger. All demonstrated high affinity binding to the paracrine signals identified and with high levels of receptors in FLCs and in their normal controls,

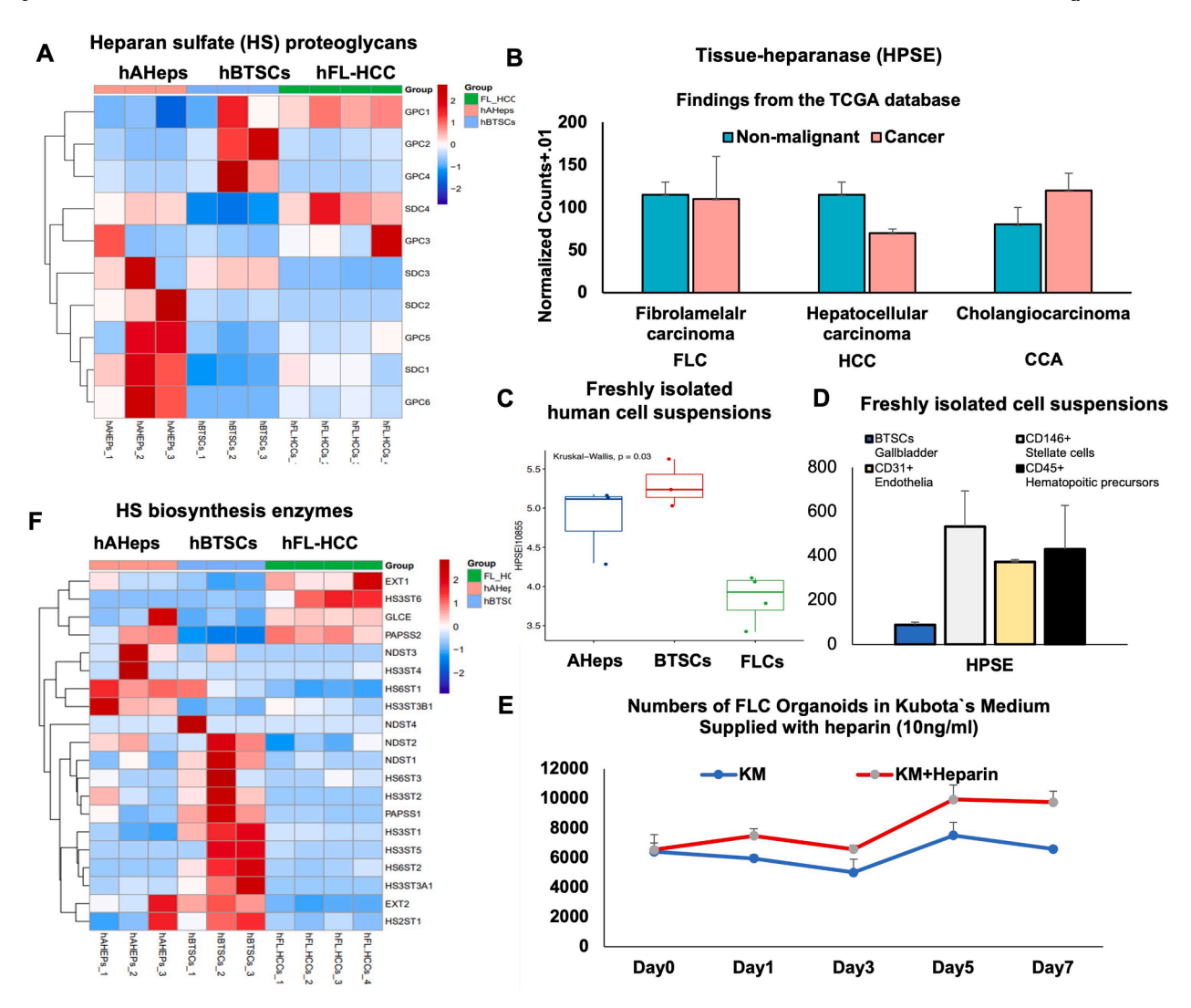


Fig. 7. Proteoglycans, Heparan Sulfate (HS) Biosynthesis, and Heparanase (HPSE).

A. A heatmap shows the expression of heparan sulfates and heparan sulfate proteoglycans (HS-PGs) relevant to hBTSCs, organoids of human biliary tree stem cells; FLCs= organoids of human fibrolamellar carcinomas (genetic signatures of transformed BTSCs) and adult hepatocytes (hAHeps) = aggregates of human adult hepatocytes (mixture of diploid and polyploid hepatocytes). Syndecans (SDCs), transmembrane heparan sulfate proteoglycans, include syndecans 1 and 4 found expressed in FLCs; Glypicans (GPCs), heparan sulfate proteoglycans bound to the plasma membrane by lipids (phosphotidyl inositol) include glypican 1 and 6 found expressed by FLCs. Expression pattern of HPSE (gene encoding heparanase) in hepatocellular carcinomas (HCC), cholangiocarcinoma (CCA), and FLCs versus normal tissue. The findings are from the TCGA database.

- B. RNA-seq data of expression patterns of HPSE in isolated suspensions of normal adult hepatocytes, normal biliary tree stem cells, and FLCs.
- C. RNA-seq analysis of HPSE in hepatic non-parenchymal cell populations including CD146⁺ stellate cells, CD31⁺ sinusoidal endothelia, and CD45⁺ hematopoietic cells.
- D. RNA-seq analysis of HPSE in hepatic non-parenchymal cell populations including CD146⁺ stellate cells, CD31⁺ sinusoidal endothelia, and CD45⁺ hematopoietic cells.
- E. If treated with 10 ng/ml heparins (Sigma), the organoids expanded slowly with a doubling every 7-9 days.
- F. Expression patterns of HS biosynthesis enzymes and sulfotransferase in hAHeps, hBTSCs and FLCs. The overall expression level of HS biosynthesis enzymes was low in FLCs compared to hAHeps, hBTSCs. The exostosin glycosyltransferase 1 (EXT1), Glucuronic Acid Epimerase (GLCE), 3'-Phosphoadenosine 5'-Phosphosulfate Synthase 2 (PAPSS2), as well as one isoform of 3-O-sulfotransferease, HS3ST6, were the only ones that were highly expressed by FLCs.

BTSCs.

HS microarray analysis technique was used for the screening for the binding between growth factors and HS oligosaccharides. On the chip, 53 different oligosaccharides were bound to the surface. The paracrine signals were tagged with a GFP fluorophore and were added to the chip. The binding pattern was read according to the value of the GFP signal in the chip (Fig. 8B). The oligosaccharides #18 and #19, the 2, 3, 6-O sulfated 12-mer HS oligosaccharide, showed the most significant binding to both FGF2 and VEGFA. Interestingly, #19, a 2, 3, 6-O sulfated 12-mer HS-oligosaccharide, with only one 3-O sulfation modification, demonstrated higher affinity binding than #18 with two 3-O-sulfates,

indicating that chemical variables other than 3-*O*-sulfation are relevant to the binding affinities to the paracrine signals (Table S2). In summary, the binding affinities of HS-oligosaccharides to the paracrine signals depended on their chain lengths and on distinct sulfation patterns.

Complexes influenced the doubling times of the cells in the organoids (Fig. 10)

Heparin extracts from bovine intestinal mucosa, comprised a mixture of hundreds of HS- oligosaccharides of varying lengths and chemistries; these at a concentration of 10 ng/ml, caused organoid doubling times of

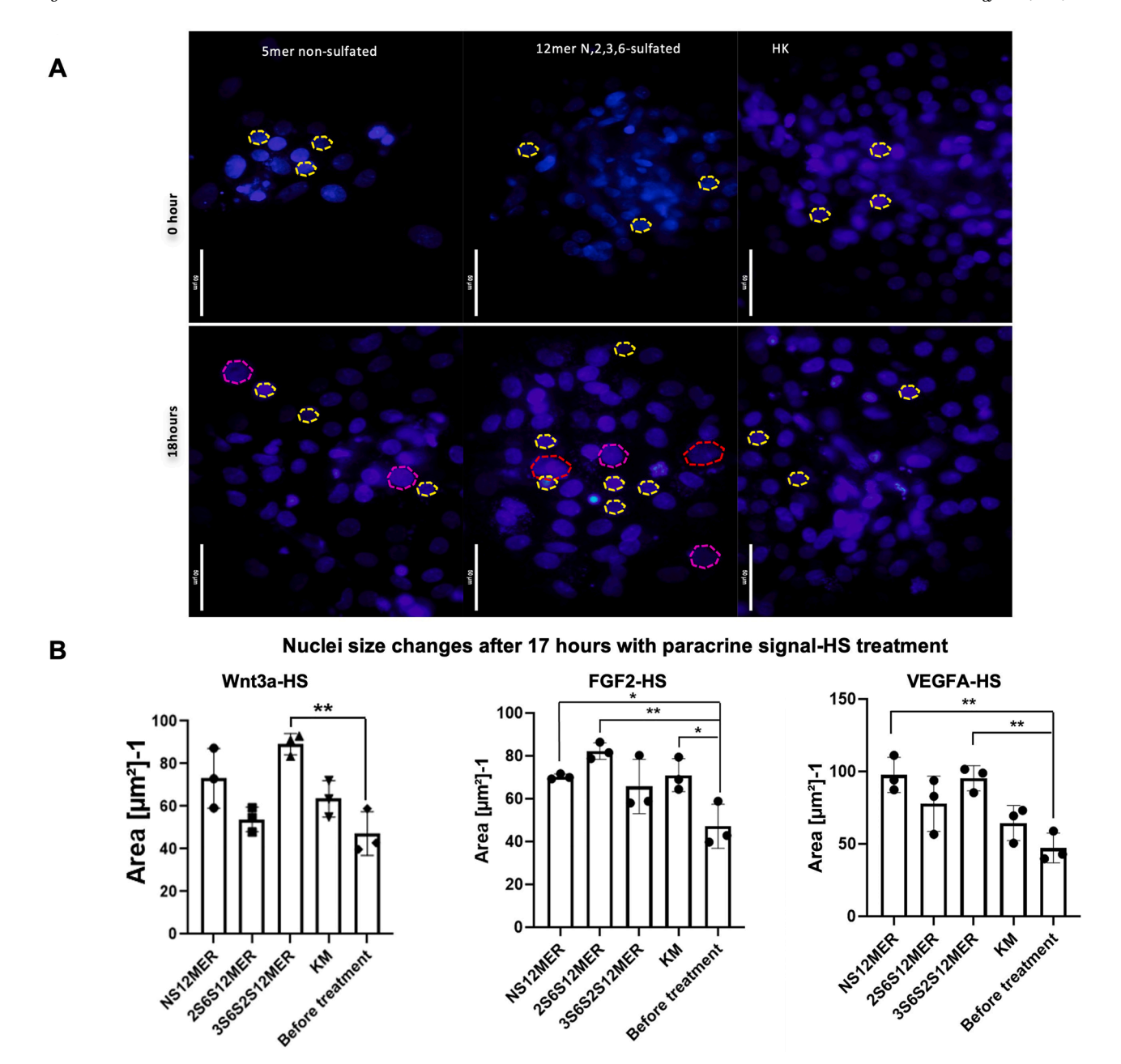


Fig. 8. Complexes of paracrine signals and synthesized HS-oligosaccharides.

A. The effects of a given complex of a paracrine signal and a HS-oligosaccharide elicited a change in the size of the nuclei of the cells within 17–18 h of treatment. Shown are cells in serum-free Kubota's Medium treated with Hoechst 33342 (2'-[4-ethoxyphenyl]-5-[4-methyl-1-piperazinyl]-2,5'-bi-1H-benzimidazole trihydrochloride trihydrate), and then the nuclei measured at time 0 and after 17–18 h of treatment with a given complex of an HS-oligosaccharide and a paracrine signal. The ones encircled in a red ring are those that are enlarged. This initial response proved an indicator of biological responses. This then became the initial screen for biological activity of complexes of synthesized HS-oligosaccharides and paracrine signals on FLCs or on BTSCs.

B. Shown are findings for Wnt3a, FGF2 and VEGF-A and specific heparan sulfate oligosaccharide chains, particularly 3S2S6S-HS 12-MERs.

~7–9 days (Fig. 7E). However, of the complexes of synthesized [HS-oligosaccharides and paracrine signals] assessed, none elicited expansion of the organoids that mimicked the findings with the heparin extracts. Rather, the complexes tested elicited slowed growth. In Figs. 10 are shown the effects of the HS complexes with three representative paracrine signals (FGF2, VEGF-A, and Wnt3a) on the doubling times of organoids of FLC-TD-2010. The 3–O sulfates complexed with the paracrine signals caused FLCs to slow in growth. The HS-oligosaccharides with 3-O sulfation complexed with Wnt3a caused the organoids to go into growth arrest comparable to the growth arrest observed in FLC spheroids and yet the aggregates remained as viable cells throughout the long period of growth arrest.

Discussion

Fibrolamellar carcinomas (FLC) are rare cancers in children, teenagers and young adults under 40 years of age and without known liver conditions associated with cancers [24,27]. Surgical resection at early stages of the disease remains the only effective treatment. A fusion gene, DNAJB1-PRKACA is a key genetic marker [21]. More recently, there have been additional mutations found relevant such as the BAP1 mutations [24,27].

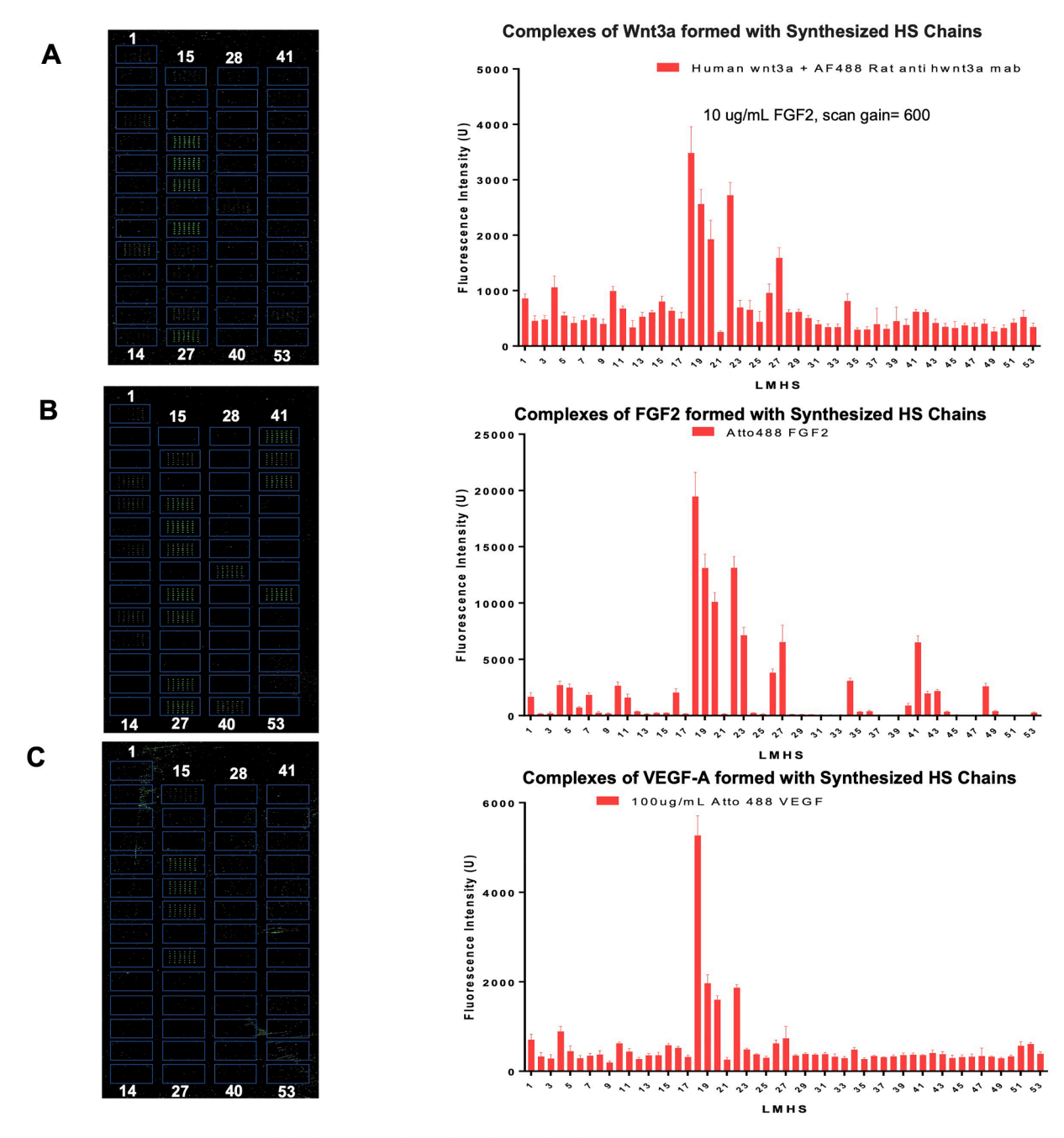


Fig. 9. Microarray assays of paracrine signals binding to synthesized HS-oligosaccharides. The binding is indicated by fluorescence (left) and the chart (right) indicates the relative binding affinity. A. Microarray layout of the binding of Wnt3a-Wnt3a antibody-Atto488.

- B. Microarray layout of the binding of FGF2-Atto 488.
- C. Microarray layout of the binding of VEGFA-Atto 488.

Stemness traits in FLCs

The first FLC-PDX model, FLC-TD-2010, established was subjected to genetic signature analyses and revealed that FLCs are genetically closest to biliary tree stem/progenitor cell populations, co-hepato/pancreatic stem/progenitor cells, found in peribiliary glands (PBGs) throughout the intrahepatic, extrahepatic and intrapancreatic biliary tree [3,19,20]. These stem/progenitor cell populations are related also to ones in the duodenal submucosal glands (dSGs), also called Brunner's glands, and pancreatic duct glands (PDGs) [5,9,17]. These stem/progenitor cell populations are known to contribute to both hepatic and pancreatic expansion and differentiation, findings that provide explanations for why some FLC tumors express either hepatic or pancreatic traits or both [3,18,19,24,27,28]. The expression by FLCs of particular ALDH isoforms, such as ALDH1A1, and low levels of others corroborated the interpretation of the FLCs as rich in stem cell traits. Figs. S1 and S2.

Using a cell line, FLX1, derived from FLC-TD-2010 PDX model, multiple groups of investigators have collaborated to show that these FLC cells have aberrant PKA signaling through Myc oncoproteins, understandings offering new options for therapeutic strategies for patients with FLCs [73].

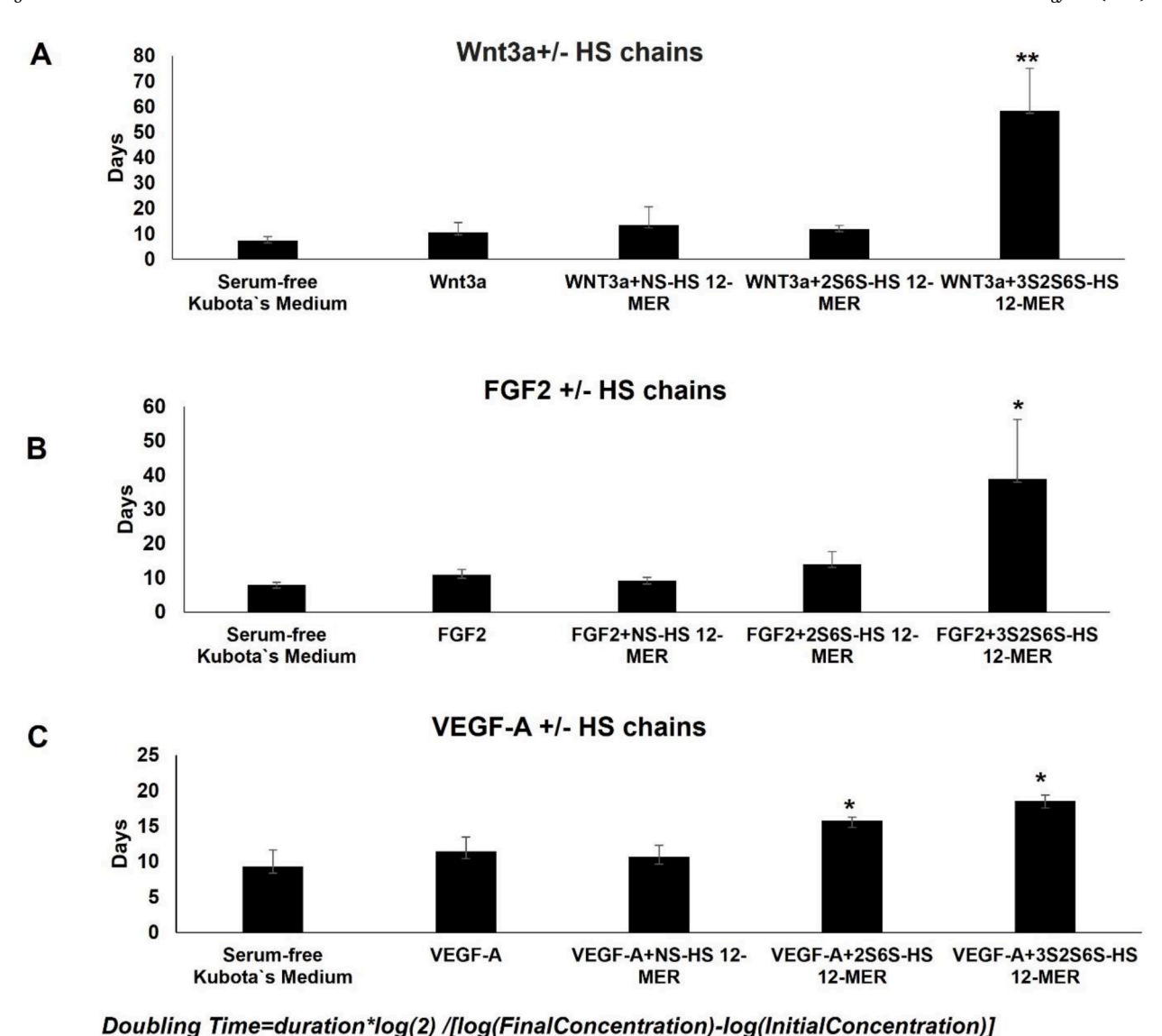


Fig. 10. Effect of complexes on growth rate of the cells in the organoids in terms of doubling times. Doubling time (in days) = duration of *log(2)/[log (final concentration)-log (initial concentration)].

Bioinformatic studies

Bioinformatic tools have helped with generating new models of FLCs from different cell types. The analyses were guided by the major stages of the network of hepato/pancreatic stem/progenitor cells contributing to hepatic and pancreatic regeneration (Figs. 4-6; summarized in Fig. S6) and defined from past studies characterizing the network of stem/progenitors and their descendants for both the liver and the pancreas [4,7, 10,91,92]. The major features of that network guided studies on pseudo-time trajectory analyses from the ArchR to assess whether FLCs are derived from recognizable hepatic lineages, including mature stages or from early-stage biliary stem cells that are precursors to both hepatic and pancreatic cells (Figs. S4 and S5). By using the Pseudo-time trajectory analysis from the ArchR, we identified transcription factor (TF) motifs for which accessibility is positively correlated with the gene expression of the corresponding TF gene (r > 0.5) when FLC tumor cells are derived from hepatocytes (Fig. S4). TFs identified include SOX4, KLF6, FOXC1 which are candidate genetic modification tools when generating FLC models from mature hepatocytes.

We attempted also to conduct a similar pseudo-time trajectory analysis on the biliary stem/progenitor epithelia to FLCs. However,

there were no BTSCs populations assigned in the six clusters we identified in Fig. S5. Because BTSCs share markers (including KRT19, Sox9, FoxA2), we hypothesized that there could be a mixture of sub-cellular populations in the original cholangiocyte clusters, which might include BTSCs. Therefore, we conducted further analyses of the original assigned cholangiocyte cluster with known BTSCs markers and small cholangiocyte markers and large cholangiocyte markers as listed in Fig. S5A. As a result, we obtained two cell clusters: cluster 1 expressed markers of small cholangiocytes (Sox9, FoxA2), while cluster 2 expressed markers of large cholangiocytes (CFTR, KRT7). No cluster that expressed BTSCs specified markers (Sox17, PDX1, Sall4, etc.) were identified. Therefore, we couldn't identify the key transcriptional factors required for the transitioning of cholangiocytes to FLCs with the current snATAC-seq datasets. As BTSCs are commonly located in the peribiliary glands in the ductal walls of the large bile ducts, we hypothesized that the FLC tumors and non-malignant tissues collected for the snATAC-seq datasets might contain limited numbers of the relevant subpopulations of BTSCs. Moreover, this is likely true given that FLCs are genetically closest to the stage 1 BTSCs (negative for both EpCAM and for LGR5 and replete with pluripotency gene expression) that have been identified in the crypts located near to the fibromuscular layer at the centers of the

bile duct walls. We assume that this is the reason that no clusters were identified in our study.

In our prior studies we had found a maturational lineage gradient in gene expression in the BTSCs starting with the most primitive ones at the innermost region of the duct walls and progressing to more mature traits with proximity to the duct lumens [7]. We hypothesize that FLCs are more likely to be transformants of the primitive subset, the stage 1 BTSCs, that are in the presumptive stem cell crypt, as indicated in Fig. S6 and less likely to be the result of dedifferentiaion of mature parenchymal cells such as hepatocytes or cholangiocytes.

Acinar cell and MMP features of FLC-TD-2010

During the characterization of organoids generated from FLC-TD-2010, FLCs were found able rapidly (within hours) to dissolve matrix substrata, even the complex liver-specific biomatrix scaffolds. Although this propensity for enzymatic dissolution and disintegration of the cultures occurred also in KM/HA, it was less than with other culture conditions enabling the organoids in KM/HA to achieve some degree of stability. We found that conditions resulting in disintegration correlated with expression by FLCs of pancreatic acinar enzymatic activity, complemented by the expression of multiple matrix metalloproteinases (MMPs) (Fig. S3). The source of MMPs derived from both FLCs and from their mesenchymal cell partners. Among the MMPs, MMP7 was significantly expressed by FLCs, an enzyme shown also expressed by smooth muscle cells [93]. MMP7 and other MMPs, such as MMP26, are commonly expressed by other cancers (e.g. prostate cancers, hepatocellular carcinomas) [94]. The release by FLCs of such enzymes has been a major cause minimizing the ability to establish FLCs ex vivo and a factor in the significant propensity for invasion and metastasis in hosts transplanted with FLC tumors.

Organoids versus spheroids reveal relevance of paracrine signaling

FLCs did not survive for more than 7–10 days if cultured in monolayers or as cell suspensions. The cells routinely detached from the dishes and underwent fragmentation. As noted above, this proved due to the release of pancreatic acinar enzymes and MMPs that caused the cultures to self-destruct. The ex vivo format that proved more stable was that of organoids, aggregates of the FLCs partnered with early lineage stage mesenchymal cells, angioblasts and precursors to stellate cells and endothelia. The organoids were maintained stably if maintained in KM, a wholly defined medium designed originally for hepatoblasts and subsequently found successful for various endodermal stem cell populations including hepatic stem cells and biliary tree stem cells[10,12,30]. The organoids, however, demonstrated some degree of cell fragmentation, due to the release of enzymes, found minimized by supplementation of the media with hyaluronans.

FLCs expressed hyaluronan receptors, a common trait for stem/progenitors [95-99]. CD44 is a 100 kDa glycoprotein widely expressed on epithelial stem/progenitors and on human leucocytes. The CD44 family is encoded by 20 exons and produces a CD44 standard body (CD44s) and CD44 variants (CD44v) through selective splicing and with the various CD44 isoforms associated with specific cell types. The FLCs expressed CD44s and two variants, CD44v3 and v10.

This provided a wholly defined, *ex vivo* FLC organoid cultures with conditions that stabilized them and enabled further explorations for factors to elicit expansion or differentiation. Slow expansion of the organoids occurred under these conditions and could be promoted if the cultures were supplemented with heparin extracts but not with any of the complexes of a synthesized HS-oligosaccharide and a paracrine signal that have been assessed thus far on FLCs. Therefore, in the future further complexes must be screened to identify those able to mimic the slow expansion of the organoids elicited by heparin extracts comprised of hundreds of distinct HS-oligosaccharides.

Other organoid models of FLCs

There are now multiple patient-derived-xenograft (PDX) models of FLC established in immunocompromised hosts [3,25] and being used to generate organoid lines in cultures for high-throughput drug screens [25]. The new FLC organoids models were generated using conditions established for hepatic organoid systems, established originally by Huch and Hu et al., respectively [100,101]. The conditions for these organoids include Matrigel, a growth factor-rich extract of a murine embryonal basement membrane tumor, in combination with myriad small molecules and growth factors [102] and a rich array of growth factors including HGF, TGFA, EGF, gastrin, FGF10, FGF7, R-Spondin I, and Wnt3a [25,102-104].

The new FLC organoid models are maintained under such wholly distinct and growth factor-rich conditions that it is improbable that they are equivalent to organoids of FLC-TD-2010 maintained in KM/HA.

An alternative hypothesis is that the new organoid models are representative of distinct subpopulations of FLCs with some being transformants of stem/progenitors to hepatic versus pancreatic versus bile duct fates. This hypothesis is consistent with the early reports from Jessica Zucman-Rossi who did genomic studies predicting a number of distinct forms of FLCs [27,28,105] and with our findings that the organoids from FLC-TD-2010 have so many pancreatic traits and few hepatic ones [3]. It will be extremely interesting to learn if these new models also have aberrant PKA signaling, as shown for FLX1 from the original PDX model [73]

Most recently, there have been efforts to transduce normal human fetal liver cells to learn the relevance of specific genes and gene combinations. The most successful of these efforts have been those of Artegiani, Hendriks and associates, who have assessed the effects of specific genes or gene combinations on organoids of fetal human liver cells, under complex culture conditions for ductular epithelia [29]. They found that the loss of BAP1 and PRKAR2A resulted in cells with traits closest to those of FLCs. The genetically engineered organoids are still distinct in aspects of all of the known phenotypic traits of native FLCs such as not producing the wealth of degradative enzymes associated with FLCs and of requiring quite complex culture conditions for survival and expansion. Further efforts are required to establish other FLC organoids or from newly genetically engineered ones from normal cells to learn of additional genes relevant to the known properties of FLCs.

The significance of desmoplasia in FLCs: relevance to paracrine signaling

A key feature of all FLCs is their extensive desmoplasia and the abundant production of exosomes [2,3,24]. This trait was observed in the first FLC-PDX model, FLC-TD-2010, and now in the new FLC-PDX models [3,25]. Importantly, the desmoplasia is correlated with paracrine signaling regulation and found to be essential for expansion of FLCs as indicated by the absence of expansion in spheroids versus its occurrence in organoids. Key paracrine signals identified included FGF2, VEGF, Wnt7b, HGF, EGF, IL6, IL11, and LIF. By checking the gene expression levels of these growth factors and their receptors in FLC organoids, we found that most are expressed at very low levels in FLCs, but the receptors for them are expressed at high levels (e.g. MET, HGF receptor; EGFR, TGFa/EGF receptor; LGR5, R-spondin-receptor) (Figs. 3-6).

Direct proof of desmoplasia's importance in FLC tumors' growth was made evident in depletion of the mesenchymal cells by immunoselection to generate spheroids, resulting in growth arrest of the FLCs. Expansion was restored with co-cultures of the FLCs with mesenchymal cell precursors and at particular ratios (e.g. 7:3). Analyses of the sources of the paracrine signals indicate that they derive from precursors to endothelia and to stellate cells that are associated with the FLC tumor cells.

The mesenchymal cell precursors also proved critical as sources of particular glycosaminoglycans (GAGs), including hyaluronans, chondroitin sulfates and heparan sulfates [3,24,39]. The hyaluronan

receptors expressed by FLCs include ones such as CD44v3, known as a heparan sulfate-binding variant [106]. Noteworthy was FLCs' very low level of expression of heparanase relative to that observed with BTSCs and by adult hepatocytes. The significance of this is not yet understood.

Biological effects of complexes

Hyaluronans, chondroitin sulfates, and heparan sulfates are expressed by both mesenchymal and epithelial stem cells. Although the biosynthetic genetic "machinery" for synthesis of heparan sulfates is found in the FLCs and BTSCs, their levels of expression are low. The first evidence of significant levels of minimally sulfated heparan sulfates associated with the maturational lineages of normal hepatic epithelia is in hepatoblasts, descendants of hepatic stem cells and found near or in the canals of Hering. More complex forms of heparan sulfates have been found associated with committed hepatic progenitors and mature hepatic parenchymal cells [49,89,107-111]. This is in contrast to our findings in prior studies in which biosynthesis of chondroitin sulfates and expression of particular chondroitin sulfate (CS) proteoglycans, such as vascular cell adhesion molecule-1 or Versican (VCAN), are highly elevated in FLCs. Thus, we hypothesize that proliferation rates of FLCs might be influenced significantly by chondroitin sulfates (CS), by CS-proteoglycans and by complexes of CSs and paracrine signals, an hypothesis now under assessment.

As noted above, we did not find any complexes of a paracrine signal and a synthesized HS-oligosaccharide that elicited expansion of the organoids, a finding that we assume means that there are other HSoligosaccharides partnered with a paracrine signal(s) yet to be identified given the growth-promoting effect of heparin extracts (containing hundreds of distinct HS-oligosaccharides). Instead, we observed striking inhibition of growth of the FLC organoids with paracrine signals in complexes with 3-O sulfated heparan sulfate chains (Figs. 8-10). Complexes of heparan sulfate oligosaccharides, especially the 3-O sulfated oligosaccharides, and paracrine signals influenced the doubling times of the organoids, causing significant slowing of them or even cessation of growth, but without loss of viability. Of the paracrine signal/HSoligosaccharide complexes studied, that of the complex of [Wnt 3a /3-O sulfated HS-oligosaccharide] was the most potent causing the cells to go into long-term (months) growth arrest and without loss of viability of the cells. Since this form of Wnt is expressed minimally by FLCs, it will be interesting to learn if the Wnt ligands that are highly expressed in FLCs, such as Wnt7b and WNT4, will be even more potent. Those forms of Wnt ligands were not available for experimental studies and so implicate important options for future experiments.

Effects of complexes of paracrine signals and synthesized HSoligosaccharides on nuclear sizes

The biologically active complexes of paracrine signals and synthesized HS-oligosaccharides were found to trigger significant enlargement of the nuclei within 17–18 h in organoids of BTSCs and of FLCs (Fig. 8). Indeed, this proved a logical initial assay given the strict correlation we found between nuclear size changes and biological responses. We assume this to be complementary to the findings of Sanderson and associates, who demonstrated translocation to the nuclei of receptors involving HS/signal complexes [87,88,112]. Therefore, we hypothesize that complexes are being internalized and transported to the nuclei with considerable speed (hours) and resulting in significant changes (such as unwinding of the chromatin) causing nuclear size changes. Even though our findings are consistent with theirs, we do not yet have additional findings that can help elucidate the phenomena other than to conclude that it is occurring. These findings are clearly ones to be addressed in future studies.

The significance of 3-O-sulfated heparan sulfates

The sulfation at the 3-OH position of GlcN is a rare modification. This

sulfation modification results in a subpopulation of 3-O-sulfated HS, closely related to biological functions [113]. For example, 3-O-sulfation is the key structural motif for the anticoagulant activity of HS and pharmaceutical heparins, the drugs used to treat clotting disorders [65]. Furthermore, 3-O-sulfated HSs serve as an entry receptor for herpes simplex virus-1 [114], the regulation of axon guidance and growth of neurons [115] as well as control of the progenitor cell expansion for salivary gland development [89]. The distinct biological functions from 3-O-sulfated HS are attributed to different saccharide sequences around the 3-O-sulfated GlcN residue [90,116]. Analyses of Matrigel have revealed that there are no 3-O-sulfated heparan sulfates evident in Matrigel [113]. Therefore, it is not surprising that the responses to Matrigel by FLC organoids were so distinct from those from use of synthetic 3-O-sulfated HS-oligosaccharides partnered with various paracrine signals.

Potential for chemotherapy for FLCs

There is an exciting prospect of using the synthesized HS-oligosaccharides for targeted therapies of FLCs. Unlike classical signal transduction pathways triggered by proteins, those regulated by heparan sulfates cannot be escaped by switching to alternate signaling pathways. Moreover, as noted above, synthetic heparan sulfate oligosaccharides can be prepared that are resistant to heparanase and the customary breakdown mechanisms and so stabilized in their effects *ex vivo* and *in vivo*. In summary, the findings of potent effects on tumor growth *ex vivo* by [paracrine signal/HS-oligosaccharides] complexes offer an exciting potential for future chemotherapeutic uses on their own or as adjuvants to other therapies.

Experimental procedures (Materials and Methods)

Companies providing reagents and supplies: Abcam, Cambridge, MA; ACD Labs, Toronto, CA; Acris Antibodies, Inc), San Diego, CA; Advanced Bioscience Resources Inc) (ABR), Rockville, MD; Agilent Technologies, Santa Clara, CA; Alpco Diagnostics, Salem, NH; BD Pharmingen, San Jose, CA; Becton Dickenson, Franklin Lakes, NJ; Bethyl Laboratories, Montgomery, TX; BioAssay Systems, Hayward, CA; Cambridge Isotope Laboratories, Tewksbury, MA; Biotime, Alameda, CA; Carl Zeiss Microscopy, Thornwood, NY; Carolina Liquid Chemistries, Corp., Winston-Salem, NC; Charles River Laboratories International, Inc), Wilmington, MA; Chenomx, Alberta, Canada; Cole-Parmer, Court Vernon Hills, IL; DiaPharma, West Chester Township, OH; Fisher Scientific, Pittsburgh, PA; Gatan, Inc), Pleasanton, CA; Illumina, San Diego, CA; Ingenuity, Redwood City, CA; Life Technologies Corp., Grand Island, NY; Leica, Washington, DC; Life-Span Biosciences, Inc), Seattle, A; Molecular Devices, Sunnyvale, CA; Olympus Scientific Solutions Americas Corp., Waltham, MA; PhoenixSongs Biologicals (PSB), Branford, CT; Polysciences, Inc), Warrington, PA; Qiagen, Germantown, MD; R&D Systems, Minneapolis, MN; RayBiotech, Norcross, GA; Santa Cruz Biotechnology, Inc), Dallas, TX; Sigma-Aldrich, St. Louis, MO; Tousimis Research Corp., Rockville, MD; Triangle Research Labs (TRL), Research Triangle Park, NC; Umetrics, Umea, Sweden; Varian Medical Systems, Inc), Palo Alto, CA; Vector Laboratories, Burlingame, CA; VWR Scientific, Radnor, PA)

General comments

The methods and procedures are comprised of both routine procedures (e.g. histology) that have been standardized for decades plus more current methods (e.g. RNA-seq) for which we have been among those helping to establish the methods. To minimize the need for investigators to have to retrieve each of the publications in which the more current methods are first presented, we have provided the reference(s) for the publication(s) in which the methods were first used and then

have provided a summary of the methods as given below.

Sourcing of normal human tissue

Adult, normal, human biliary tissues were dissected from tissue connected to intact livers and pancreases obtained but not used for transplantation into a patient. They were obtained through organ donation programs via United Network for Organ Sharing (UNOS). Those used for these studies were considered normal with no evidence of disease processes. Informed consent was obtained from next of kin for use of the tissues for research purposes, protocols received approval from the Institutional Review Board for Human Research Studies (#97–1063) at UNC at Chapel Hill, NC, USA.

Human samples of fibrolamellar carcinomas

Informed consent was obtained from all individuals. Tumor and adjacent non-malignant liver samples were collected from patients with FLC by surgeons in accordance with the Institutional Review Board protocols 1802007780, 1811008421 (Cornell University) and 33970/1 (Fibrolamellar Cancer Foundation). They were provided by the Fibrolamellar Cancer Foundation. Patients included male and female subjects, and in some cases multiple samples were collected from the same patient. All samples were de-identified before shipment to Cornell or to UNC.

Animals

Immunocompromised mice, NOD.Cg-Prkdcscid Il2rgtm1Wjl/SzJ (NSGs), both male and female, and all of them 4–6 weeks of age, were obtained from breeding colonies on the UNC campus and used as hosts for the tumor cells. These mice are devoid of T or B cells, lack functional NK cells and are deficient in cytokine signaling. The strain combines the features of the NOD/ShiLtJ (Stock Number 001976) background, the severe combined immune deficiency mutation (SCID, which is caused by a spontaneous mutation in the Prkdc gene), and the IL2 receptor gamma chain deficiency.

The animals were maintained in the quarters maintained by the Division of Laboratory Animals at UNC. Procedures were performed according to protocols approved by the UNC School of Medicine at Chapel Hill Institutional Animal Care and Use Committee. The IACUC approval numbers were #16–316 and #17–225. All were housed in UNC's Division of Laboratory Animals sterile facility in micro-isolated autoclaved cages with free access to autoclaved water and radiation sterilized food.

Origins of the fibrolamellar carcinoma tumor line (PDX model), FLC-TD-2010

The tumor line was established previously and has been extensively characterized [3,18-20,24,117,118] . It was established from freshly isolated ascites tumor cells that were plated onto culture dishes and in serum-free Kubota's Medium supplemented with 0.1% hyaluronans, KM/HA [3,30,67]. The FLC cells that were culture selected in serum-free KM/HA and supplemented with 50 ng/ml each of HGF and VEGF were transplanted subcutaneously in NSG mice. The culture selection process required only approximately a week. These were transplanted and formed the initial tumors but only after almost 9 months in vivo [3]. Passaging of the tumors resulted in faster appearances of flank tumors that could be passaged thereafter after ~10-12 weeks. Although the tumors formed also in the absence of hyaluronans and of the growth factors, they did so more slowly and sometimes not at all. Therefore, hyaluronans and paracrine signal supplementation were used routinely; eventually we converted to use of hyaluronan hydrogels [32,119,120]. If transplanted intraperitoneally, the tumor cells spread onto the serosal surfaces of tissues and organs throughout the peritoneum and into the liver and pancreas; the hosts did not survive for as long as when flank

tumors were generated; less than 4 weeks was typical for the life span of these mice transplanted intraperitoneally. Collecting the abdominal tissue onto which the FLC tumor cells had spread from intraperitoneal injections and processing it proved more onerous than the flank tumors, so the tumor line was maintained primarily as flank tumors.

Tissue processing of the FLC tumors, as established previously [3] to generate cell suspensions for $ex\ vivo$ studies, was conducted in RPMI 1640 supplemented with 0.1% bovine serum albumin (BSA), 1 nM selenium and antibiotics. Enzymatic processing buffer contained 600 U/ml type IV collagenase and 0.3 mg/ml deoxyribonuclease at 32 °C with frequent agitation for 15–20 min. Enriched suspensions were pressed through a 75-gage mesh and spun at 1200 rpm for 5 min before re-suspension. Estimated cell viability by trypan blue exclusion was routinely >95%. These methods were established in the original studies on FLCs [3].

Magnetic immunoselection of FLC cells

Human tumor cells were isolated from xenografted FLC tumors as described previously [3] with some modifications. Negative sorting was done using EasySep magnetic bead immunoselection using the magnetic cups and beads (StemCell Technologies, Vancouver, Canada) and according to the manufacturer's instructions. Briefly, the dissociated cells were washed in phosphate-buffered saline (PBS) and were treated with FcR blocking antibody and incubated with a cocktail of biotin-conjugated anti-mouse antibody against lineage cells (1:10 dilution, Miltenyi Biotech, Auburn, CA) and with biotin-conjugated anti-mouse-MHC class I (H2Kd; clone SF1-1.1, 1:100 dilution) and CD31 (clone MEC13.3, 1:100 dilution) antibodies (BD Biosciences, San Jose, CA) at room temperature for 15 min. Cells were incubated with the biotin selection cocktail for 15 min, and then incubated with magnetic nanoparticles at room temperature for 10 min. The cups were magnetized, and cells or clumps of cells bound to the walls of the cup; those not bound (the human cells) were collected into a separate container. The cells bound to the cups were the mouse cells that were discarded. The human cells were suspended in Kubota's Medium (KM) and then plated. The cells were plated onto culture plastic or on or in hyaluronan hydrogels and provided with serum-free KM/HA. For the initial plating, the medium was supplemented with 2% FBS (HyClone, Waltham, MA). After a few hours, the medium was changed to the serum-free KM/HA, and this was used for all subsequent medium changes. For the cultures from xenografted tumors, the human cells were sorted by immunoselection away from the murine (host) mesenchymal cells and then were plated in serum-free KM/HA from the outset.

Culture media and solutions

The choices of media and supplements derived from prior studies on maintenance of cells under wholly defined conditions [7,16,67,121]. All media were sterile filtered (0.22 μm filter) and kept in the dark at 4°C before use. Basal medium and fetal bovine serum (FBS) were purchased from GIBCO/Invitrogen. All growth factors were purchased from R&D Systems. Hyaluronans were obtained from Glycosan Biosciences (Salt Lake City, Utah; formerly a subsidiary of Lineage Cell Therapeutics (Alameda, CA), and are now offered in non-clinical grade form from Advanced Biomatrix (Carlsbad, CA) and in the clinical grade form from Sentrex Animal Care (Salt Lake City, UT) (G. Prestwich, personal communications). All other reagents, except those noted, were obtained from Sigma.

Cell wash

The cell wash conditions were developed for isolation of stem/progenitors from various tissues as described previously [12,92,121]. Cell wash was comprised of 599 mls of basal medium (RPMI1640; Gibco # 11875–093), supplemented with 0.5 gs of serum albumin (Sigma, #

A8896–5 G, fatty acid free), 10^{-9} M selenium, 5 mls of antibiotics (Gibco #35240–062, AAS). It was used for washing tissues and cells during processing.

Collagenase buffer

As defined in prior studies, collagenase preparations were used for isolation of cells [7,12,67]. It consists of 100 mls of cell wash supplemented with collagenase (Sigma # C5138) with a final concentration of 600 U/ml (R1451 25 mg) for biliary tree (ducts) tissue and 300 U/ml (12.5 mg) for organ-parenchymal tissue (liver, pancreas)

Kubota's Medium (KM)

KM is a serum-free medium designed originally for rodent hepatoblasts [30,67]. and found effective also for all determined endodermal stem/progenitors assayed including human hepatoblasts and for human hepatic, pancreatic and biliary tree stem cells and progenitors [6,7,12,16]. It consists of any basal medium (here being RPMI 1640) with no copper, low calcium (0.3 mM), 10^{-9} th M selenium, 0.1% BSA, 4.5 mM nicotinamide, 10^{-12M} , zinc sulfate heptahydrate, 10^{-8M} hydrocortisone, 5 µg/ml transferrin/Fe, 5 µg/ml insulin, 10 µg/ml high density lipoprotein and a mixture of purified free fatty acids added after binding to purified human serum albumin. The detailed protocol for the preparation of KM has been given in a review of methods [121]. KM is available commercially from *PhoenixSongs Biologicals* (Branford, CT).

Hormonally defined media (HDM)

Supplements can be added to Kubota's Medium to generate a serumfree HDM that will facilitate differentiation of the normal stem cells (e.g. HpSCs or BTSCs) [7-10,16] . These HDM cause stable differentiation of the normal stem cells [7,16,67], but transient differentiation of the FLCs in culture. FLCs in monolayers in HDM last a few days to a week after which the cells reverted to ones detaching from dishes and with enhanced stem cell traits [3]. The HDM included supplementation with calcium to achieve at or above 0.6 mM concentration, 1 nM tri-iodothyronine (T3), 0.1 nM of copper, and 20 ng/ml of FGF2 to generate a modified Kubota's Medium (MKM). As reported in studies on normal stem cells [16], the medium conditions over and above these and needed to selectively yield hepatocytes (HDM-H) versus cholangiocytes (HDM-C) versus pancreatic islets (HDM-P) [of the normal stem cells]

HDM-H: MKM supplemented further with 7 μ g/ml glucagon, 2 g/l galactose, 10 ng/ml epidermal growth factor and 20 ng/ml HGF. **HDM-C:** MKM supplemented further with 20 ng/ml VEGF 165 and 10 ng/ml HGF.

HDM-P: The MKM is prepared without glucocorticoids and further supplemented with 1% B27, 0.1 mM ascorbic acid, 0.25 mM cyclopamine,1 mM retinoic acid, 20 ng/ml of FGF-7 for 4 days, then changed with one supplemented with 50 ng/ml exendin-4 and 20 ng/ml of HGF for 6 more days of induction.

Preparation of normal human cell suspensions

In methods established previously, we isolated stem cells from biliary tree tissue [7,10,11,122]. Extrahepatic biliary tree tissues (gall-bladder, common duct, hepatic ducts) were dissected from human tissues isolated for organ transplantation (liver, pancreas) but then not used and made available for research. Tissues were pounded with a sterilized, stainless-steel mallet to eliminate the parenchymal cells, carefully keeping the linkage intact of the intrahepatic and extrahepatic bile ducts. The biliary tree was then washed with the "cell wash" buffer comprised of a sterile, serum-free basal medium supplemented with antibiotics, 0.1% serum albumin, and 1 nM selenium (10^{-9} M). It was

then mechanically dissociated with crossed scalpels, and the aggregates enzymatically dispersed into a cell suspension in RPMI-1640 supplemented with 0.1% bovine serum albumin (BSA), 1 nM selenium, 300 U/ml type IV collagenase, 0.3 mg/ml deoxyribonuclease and antibiotics. Digestion was done at 32°C with frequent agitation for 30–60 min. Most tissues required two rounds of digestion followed by centrifugation at 1100 rpm at 4 °C). Cell pellets were combined and re-suspended in cell wash. The cell suspension was centrifuged at 30 G for 5 min at 4 °C to remove red blood cells. The cell pellets were again re-suspended in cell wash and filtered through a 40 μ m nylon cell strainer (Becton Dickinson Falcon #352340) and with fresh cell wash. The cell numbers were determined, and viability was assessed using Trypan Blue. Cell viability above 90–95% was routinely observed.

Early mesenchymal cell precursors needed as partners with the epithelia in organoids

In prior studies, we defined the antigenic profile of populations of mesenchymal cells that provide critical paracrine signals needed for hepatic and biliary tree stem cells versus others required for mature parenchymal cells [7,16,76] The mesenchymal cells needed for BTSCs and for the FLCs are subpopulations devoid of or with minimal MHC antigens, with low side scatter, and identifiable as angioblasts (CD117⁺, CD133⁺, VEGF-receptor⁺, and negative for CD31), precursors to endothelia (CD133⁺, VEGF-receptor⁺, and CD31⁺), and precursors to stellate cells (CD146⁺, ICAM1⁺, VCAM⁺, alpha-smooth muscle actin (ASMA)⁺, and negative for vitamin A) [76,77]. We will refer to these 3 subpopulations as early lineage stage mesenchymal cells (ELSMCs) comprised of angioblasts and their early lineage stage descendants, precursors to endothelia and to stellate cells. By contrast, adult hepatocytes are associated with mature sinusoidal endothelia (CD31++-VEGF-receptor⁺, type IV collagen+ and negative for CD117); those for adult cholangiocytes are associated with mature stellate and stromal cells (ICAM-1⁺, ASMA⁺, Vitamin A⁺⁺, type I collagen⁺).

FLC spheroid formation

Spheroids are floating aggregates of just the FLCs, that is tumor cell suspensions depleted of or with minimal mesenchymal cells. For spheroid formation assays, 1×10^4 FLC cells, depleted of host mesenchymal cells by magnetic sorting, were seeded into each well of a sixwell plate coated with Ultra-Low Attachment surfaces (Corning, Lowell, MA) and cultured with serum-free Kubota's Medium in the presence of 1 mg/ml hyaluronans (Sigma, St Louis, MO), referred to as KM/HA. For secondary spheroid formation, mesenchymal cells sorted by magnetic sorting, were seeded into each well of a 12-well plate, coated with 5 mg/cm hyaluronan and cultured with KM plus 2% FBS overnight. After 16-20 h, the cells were incubated for 7 days with either serum-free KM/HA (as the undifferentiated control) or with serum-free HDM-H, HDM-C or HDM-P. After a total of 7 days of culture, cells were harvested for analyses of gene expression assays, the primary spheroids were collected and then dissociated with NeuroCult Chemical Dissociation Kit (StemCell Technologies, Vancouver, BC, Canada). Cell suspensions were centrifuged at 700 rpm for 10 min and resuspended in KM/HA. After 2 weeks, the number of spheroids (size $= >100 \ \mu m$) were counted. Differentiation assays. For these assays, 1×10^5 FLCs, depleted of mesenchymal cells, were seeded onto low attachment dishes and allowed to form spheroids that were then provided with either HDM-H versus HDM-C or HDM-P. The cultures were maintained for 7 days and then analyzed.

Organoid formation (of FLCs or BTSCs)

The cell suspensions were added to Multi-well Flat Bottom Cell Culture Plates (Corning #353,043) in serum-free Kubota's Medium and incubated for \sim an hour at 37°C to facilitate attachment of mature

mesenchymal cells; the mature stroma attached to the dishes within 10–15 min even though the medium was serum-free. The cells remaining in suspension were transferred to another dish and again incubated for up to an hour. Repeats of this resulted in depletion of a significant fraction of the mature mesenchymal cells. After depletion of mature stroma, the remaining floating cells were seeded at $\sim\!2\times10^5$ cells per well in serum-free KM onto Corning's ultralow attachment dishes (Corning #3471) and were incubated overnight at 37°C in a CO2 incubator. Organoids comprised of the biliary tree stem cells (BTSCs) partnered with ELMSCs formed overnight (Fig. 1 and Figure S1). Organoids can be maintained indefinitely in serum-free KM/HA and for these studies lasted months and for the key experiments were sustained for more than 2 months.

Organoids could be converted to primary monolayer cultures by plating them into 6-well cell culture plates coated with collagen III or collagen IV. If the organoids were prepared from FLC tumor cells, the monolayer cultures were transient and converted back to floating cells within a few days; the organoids of normal stem cells (e.g. BTSCs) gave rise to healthy, epithelial monolayer colonies especially if on substrata of collagens or hyaluronan hydrogels.

The addition of 1 mg/ml HA in the medium improved the maintenance of the FLC organoids for at least 2 months or longer; this finding is logical given that the cells strongly express multiple CD44 isoforms.

Hyaluronans (HAs)

Soluble, long chain forms of HA (Sigma Catalog # 52747) were used in stabilization of organoid cultures and in cryopreservation of cells [123,124]. Those used to make the hydrogels, thiol-modified HAs, were obtained from Glycosan Biosciences, formerly a subsidiary of Lineage Cell Therapeutics (Alameda, CA), and now are offered in non-clinical grade form from Advanced Biomatrix (Carlsbad, CA) and in the clinical grade form from Sentrex Animal Care (Salt Lake City, UT) (G. Prestwich, personal communications). The components for these thiol-modified HAs were made by a proprietary bacterial-fermentation process using bacillus subtilis as the host in an ISO 9001:2000 process (www.biopolymer.novozymes.com/)[125-128]. The components were produced by Novozymes under the trade name, HyaCare®, and are 100% free of animal-derived materials and residual organic solvent. No animal-derived ingredients are used in the production, and there are very low protein levels and no endotoxins. The production follows the standards set by the European Pharmacopoeia. The HA hydrogels were prepared using Glycosil (HyStem® HAs, ESI BIO-CG313), the thiol-modified HAs, that can be triggered to form disulfide bridges in the presence of oxygen, or by forming thio-ether linkages using polyethylene glycol diacrylate (PEGDA). Glycosil® is reconstituted as a 1% solution of thiolated HA in 1% phosphate buffered saline (PBS) using degassed water, or, in our case, in serum-free Kubota's Medium. Upon reconstitution, it remains liquid for several hours but can undergo some gelation if exposed to oxygen. More precise gelation occurs with no temperature or pH changes if Glycosil is treated with a cross-linker such as PEGDA causing gelation to occur within a few minutes[128-130].

We learned to make use of hyaluronan hydrogels that facilitated stability of the organoids $ex\ vivo\ [120]$. The level of cross-linking is the main contributor to the level of stiffness, or rigidity, and can be controlled by adjusting the ratio of the thiol-modified HAs to PEGDA. In prior studies, stem cell populations were tested in HA hydrogels of varying level of rigidity and were found to remain as stem cells, both antigenically and functionally (e.g. with respect to ability to migrate), but only if the level of rigidity was about or less than $\sim 100\ Pa\ [32,120,131]$.

Flow cytometric analyses

The dissociated cells were incubated at 4°C for 30 min with fluorescein isothiocyanate-conjugated or biotin-conjugated anti-mouse-MHC class I (against H2Kd; clone: 34–1–2S) (eBioscience, San Diego, CA) or anti-

human antibodies (Table 1) for cell surface markers. Antibodies used are listed in Table 1. The labelled cells were washed with permeabilization buffer, and then analyzed by FACSCalibur (BD Biosciences).

Cryopreservation of organoids

Efforts to cryopreserve the organoids were <u>not</u> successful. By contrast, the cell suspensions depleted of mature mesenchymal cells (and yet retaining the mesenchymal cell precursors) were able to be cryopreserved using conditions that we established previously [123] enabling the organoids to be prepared from freshly thawed cell suspensions. Isolated stem cell mixtures were cryopreserved in either Cryostor10 (Biolife, Seattle, WA or Stem Cell Technologies, Canada) or serum-free Kubota's Medium supplemented with 10% DMSO at $3{\sim}4\times10^6$ cells per vial. Their viability was improved by further supplementation with 0.1% HAs (Sigma #52747). Cryopreservation was done using CryoMedTM Controlled-Rate Freezers. The viability on thawing was greater than 90%. The cryopreservation conditions were developed previously and are successful for hepatic stem cells, biliary tree stem cells and hepatoblasts [123,124].

Characterizations of organoids

Histology

After 48+ hours of fixation, organoids were placed in labelled cassettes in 70% ethanol and were processed on a long cycle at 60 $^{\circ}$ C in a Leica ASP300S Tissue Processor for approximately 10 h. After completion of the overnight processing, samples were embedded using the Leica EG1160 Embedding Station. The block was sectioned at 5 μ m using a Leica RM2235 Microtome; the sections were floated in the water bath and placed onto slides. The slides were allowed to air dry overnight before staining. Sections were stained for Haematoxylin and Eosin (H&E; Reagents #7211 and #7111) and Masson's Trichrome (Masson's Trichrome Stain: Blue Collagen Kit# 87019) using Richard Allan Scientific Histology Products and following the manufacturer's recommended protocol; the protocol is programed into a Leica Autostainer XL. Antibodies are listed in Table 1. The methods for immunofluorescence and for immunohistochemistry were established initially in prior studies on both normal and tumor tissues [7,11,12,67].

For immunofluorescent staining, frozen sections were fixed with 4% PFA for 20 min at room temperature (alternatively with acetone or methanol according to the antibody specifications). After fixation, sections were washed 3 times in 1% phosphate buffered sale (PBS), blocking with 10% goat serum in PBS (or with 2.5% horse serum in PBS) for 2 h, and rinsed. Primary antibodies diluted in 10% goat serum (or 10% horse serum) in PBS were added and incubated at 4°C for 14 h, washed, incubated for 1 h with labelled isotype-specific secondary antibodies, washed, counterstained with 4–0,6-diamidino-2-phenylindole (DAPI) for visualization of cell nuclei and viewed using a Leica DMIRB inverted microscope (Leica, Houston, TX) or a Zeiss ApoTome Axiovert 200 M (Carl Zeiss, Thornwood, NY).

For immunohistochemistry, the tissues were fixed in 4% PFA overnight and stored in 70% ethanol. They were embedded in paraffin and cut into 5 μm sections. After deparaffinization, antigen retrieval was performed with sodium citrate buffer (pH 6.0) or EDTA buffer (pH 8.0) in a steamer for 20 min. Endogenous peroxidases were blocked by incubation for 15 min in 3% H_2O_2 . After blocking, primary antibodies reacting against human but not mouse cells were used and were applied at 4 °C overnight. M.O.M immunodetection kit (Vector Laboratories, Burlingame, CA) was used for detecting primary mouse anti-human antibodies on mouse xeno-transplanted FLC tumor cells to avoid the inability of the anti-mouse secondary antibody to bind to endogenous mouse immunoglobulins in the tissue. Sections were incubated for 30 min at room temperature with ImmPRESS peroxidase-micropolymer staining kits and 3,3′-diaminobenzidine substrate (Vector Laboratories, Burlingame, CA). Sections were lightly counterstained with

Table 1
Key Resources: Antibodies.

Antibody	Host	Type	Manufacturer	Clone	Catalog#	Dilution for testing
NANOG	Rb	IgG	Peprotech	D73G4	500-P236	1/200(IHC-P, ICC-IF),
SOX2	Rb	IgG	Cell Signaling	D6D9	3579	1/50(IHC)-400(ICC-IF)
OCT4	Rb	IgG	Cell Signaling		2750	1/200(IHC), 1/400(ICC-IF)
EpCAM	Rb	IgG	Abcam	E144	ab32392	1/200 1/100(ICC-IF)
SOX17	Ms	IgG1	Abcam	3B10	ab84990	1/100(IHC-P) 1/20(ICC-IF)
SOX9	Rb	IgG	Chemicon		AB5535	1/500-2000, IHC-P 1/1000
Ki67	Rb	IgG1	Abcam	SP6	ab16667	1/100(ICC-IF)-100(IHC)
FOXA2	Rb	IgG	Abcam		ab40874	1/500
CXCR4	Rb	IgG	Abcam		ab2074	1/100(IHC-P)-500(ICC-IF)
RGS8	Rb	IgG	SantaCruz		sc-134552	1/50(IHC-ICC-IF)1/100(IHC-P)
AFP	Ms	IgG2a	SIGMA	C3	A-8452	1/100(ICC-IF) 1/500(IHC-P)
CD44	Ms	IgG2a	Abcam	F10-44-2	ab6124	1/200(IHC-P) 1/100(ICC-IF)
PDX1	Gt	IgG	R&D		AF2419	1/50
LGR5	Rb	IgG	Sigma		HPA012530	1/500IHC 1/350 ICC
Insulin	Gp	IgG	Abcam		ab195956	IHC-P, IHC-Fr
H2Kd-Biotin	Ms	IgG2a	BD	SF1-1.11	553564	1/100 (FACS)
H2Kd-FITC	Ms	IgG2a	eBioscience	34-1-28	11–5998	1/100 (FACS)

hematoxylin. Antibodies are listed in Table 1. Images were taken using Zeiss CLSM 710 Spectral Confocal Laser Scanning microscope (Carl Zeiss Microscopy).

RNA-SEQ

The RNA-seq preparations were as done in prior studies [3,18-20]. The findings from the databases were used in bioinformatic analyses to understand the expression patterns of various gene sets, including stem cell markers, ALDH-related genes, proteoglycan-related genes, matrix metalloproteinases (MMPs), and pancreatic acinar genes. BTSCs expressed pluripotency genes, endodermal transcription factors, and stem cell surface, cytoplasmic and proliferation biomarkers. Heatmap package (version 1.0.12) was adopted to visualize the gene expression patterns, and the scale parameter was "row". Only sequencing samples related to FLCs, hAHeps and hBTSCs were collected for studies in the present work.

Single-nucleus ATAC analysis

Samtools in linux was adopted to sort bam files and then bam files were converted to fragments, which were then sorted and finally used to generate tabix files. The detailed pipeline of tabix was demonstrated in a previous study [78]. A software suite for single-cell analysis of regulatory chromatin in R (ArchR [79] (https://www.archrproject.com/) was adapted for studying the source of paracrine signaling in the organoids and in the FLC tumors. The enrichment score of the transcription start site (TSS) and fragment number of each nucleus was calculated by the ArchR package (version: 1.0.1). The Seurat V4 package was also leveraged to visualize the gene score of various cell types in FLCs [132]. To confirm the cell type annotation of different clusters, we also collected canonical cell markers to identify cell types and "Dotplot" function in the Seurat package that was adopted to show gene score changes. To plot browser tracks, we leveraged the "plotBrowserTrack" function and arranged track rows from highest to lowest accessibility. After removing the batch effect using the harmony algorithm in "plotEmbedding" functions, we annotated cell-type identity to clusters. The "plotMarkerHeatmap" function was also modified and adopted to better visualize the gene expression in snATAC-seq. Furthermore, accessibility of chromatin surrounding interesting genes was depicted based on the "plot-BrowserTrack" function. Then, we also modified the source code of "getTrajectory" function, and the trajectory analyses were performed to understand the gene changes. The gene activity scores of gene sets related to MMPs, cytokines/paracrine signals (ligands/receptors) and stem cell markers were explored in various cell types identified by snATAC-seq.

Construction of user-friendly website related to BTSCs and FLCs

All data used in the present study were collected and normalized, and then uploaded to a newly constructed user-friendly website using shinyapp in R (https://wangxc.shinyapps.io/BTSCs_FLCs). The website contained data from our previous study related to BTSCs and TCGA data related to FLCs. Researchers are able quickly to explore gene expression patterns and download interesting figures conveniently, which we hope might contribute to the field of BTSC as well as FLC studies.

Chemoenzymatic synthesis of heparan sulfate oligosaccharides

The synthesis of oligosaccharides was completed according to the chemoenzymatic method published previously [133,134]. Briefly, heparosan synthase-2 (PmHS2) from Pasteurella multocida was used to elongate the monosaccharide, GlcA-pNP, to the apropriate sized backbones. The backbone was then subjected to the modification by N-sulfotransferase (NST), C₅-epimerase (C₅-epi), 2-O-sulfotransferase (2-OST), 6-O-sulfotransferase (6-OST), 3-O-sulfotransferase isoform 1 (3-OST-1) and 3-O-sulfotransferase isoform 5 (3-OST-5). Seven major steps are involved in the overall synthesis, including (elongation to add GlcNTFA), (elongation add GlcA), (detrifluorto oacetylation/N-sulfation), (2-O-sulfation/epimerization), (6-O-sulfation), and (3-O-sulfation by 3-OST-1). The enzymes were expressed in E. coli or by insect cells using baculovirus expression approach. The structures of the oligosaccharide products were confirmed by electrospray ionization mass spectrometry. The purity of all synthesized products was > 90% as determined by high resolution HPLC.

Heparan sulfate microarray analysis

Microarray printing of oligosaccharides was spatially arrayed by a S11 robotic arrayer (Scienion) onto an NHS-functionalized glass slide (Nexterion Slide H). Each compound was printed with 36 spots in a 6 \times 6 square. Each square contains 3 sets of 12 spots, with each set consisting of a different printing density (12.5, 25 and 50 μM). After printing, slides were incubated overnight at RT in a saturated (NH4)2SO4 humidity chamber (relative humidity = 81%). Unreacted oligosaccharides were removed by washing with water and unreacted NHS sites were blocked by ethanolamine (Aldrich). Slides were stored at room temperature.

Microarray slide hybridization- A 10 μ g/mL solution of fluorescently labeled protein was prepared by diluting the protein in a PBST/Tris/BSA solution (PBS, 0.05% Tween 20, 20 mM Tris, 10% BSA, pH = 7.5). The mixture (100 μ L) was placed between the arrayed glass slide and a cover slip. The hybridization was carried out for 1 hour in a

humidity chamber. The slide was washed by shaking in a PBST solution containing 1% BSA and 20 mM Tris. Lastly, the slide was rinsed with water and dried by centrifugation.

Scanning microarray slides- Hybridized slides were scanned by a GenePix Pro 4300A scanner (Molecular Devices). Slides were scanned at 488 nM and analyzed by GenePix Pro-software.

Microarray Binding Affinity- Positive hits as determined by the initial screen were spatially arrayed in a format compatible with a 16 well-FAST slide incubation chamber (GVS Filter Technology). Then 50 μM of oligosaccharides (7 compounds for AT and 29 compounds for FGF2) were printed 14 times per slide in the same layout. The inactive areas of the slide were blocked with ethanolamine as before. 100 μL of fluorescently labeled protein (0–4 μM , 2-fold serial dilutions, i.e. 4 μM , 2 μM , 1 μM ... 4 nM, 2 nM, 1 nM, 0 nM) was pipetted into individual wells and allowed to incubate for 1 hour. The protein solution was gently washed with water, then PBST containing 1% BSA, then rinsed with water again and dried by centrifugation. The plate was read as before, and the average fluorescence intensity was plotted against the concentration of the fluorescently labeled protein.

Statistical analysis

Statistically significant differences between samples were calculated by using Student's 2-tailed *t*-test. P values of less than 0.05 were considered statistically significant. Graphs were generated in the R software package and error bars represent the standard error.

Contributions by the authors

Wencheng Zhang, PhD (wencheng.v.zhang@outlook.com or wencheng_zhang@tongji.edu.cn) was the primary investigator for the bench experiments on the FLC and BTSC studies and worked with all of the others in the various characterizations and analyses. He also spearheaded the writing of all of the stages of the manuscript.

Yongmei Xu, PhD (yongmeix@email.unc.edu) conducted the synthesis of the heparan sulfate oligosaccharides.

Xicheng Wang, MD (wangxicheng@tongji.edu.cn) and Guoxiu Wu (2131449@tongji.edu.cn), who are supervised by Zhiying He, PhD (zyhe@tongji.edu.cn). Both did bioinformatic analyses using the RNA-seq data generated by Praveen Sethupathy. A separate databank was prepared and used along with the TCGA data for the expression pattern of pancreatic enzymes and matrix metalloproteinases.

Tsunekazu Oikawa, MD (oitsune@jikei.ac.jp) and Eliane Wauthier managed the characterization of the original FLC tumors. Many of their findings were reported In the first paper on the tumor line [3,68]. In these studies, Dr. Oikawa did the assays on effects of hyaluronans on the stability and proliferation of FLCs.

Eliane Wauthier, MS– two master's degrees, one in organic chemistry and one in molecular biology (elwauthier@gmail.com). Lab management and overall supervision. Primary investigator for the methods of isolation of the stem cells and for organoid formation. She established the PDX model of FLC-TD-2010 and identified optimal ex vivo conditions for it.

Praveen Sethupathy, PhD (praveens@cornell.edu or pr46@cornell.edu) and his staff utilized tissue samples and isolated cell populations prepared by the Reid lab to do RNAseq analyses and genetic signature studies. The results were used to establish a data bank that was used for the bioinformatic analyses

Guowei Su, PhD (guowei.su@glycantherapeutics.com) did the heparan sulfate microarray analysis.

Zhiying He, PhD (zyhe@tongji.edu.cn) directed and managed the bioinformatics research and bioinformatic analyses using the RNA-seq data generated by Praveen Sethupathy.

Jian Liu, PhD (liuj@email.unc.edu) supervised all studies on synthesis and characterization of heparan sulfate oligosaccharides.

Lola M. Reid, PhD (Lola.M.Reid@gmail.com or stemcell@med.unc.

edu) managed experimental designs of the biological assays; management and supervision of the research overall; and writing plus editing of all drafts of the manuscript.

Declaration of Competing Interest

Y. Xu and J. Liu are co-founders of Glycan Therapeutics. G. Su is an employee at Glycan Therapeutics. Other authors declare no competing interests.

Data availability

Previously published RNA-seq data can be downloaded from the Gene Expression Omnibus (GEO) with the GEO accession number (GSE181922). The recently published snATAC-seq data was downloaded from GSE202315. We also visualized gene profiles in website constructed by Praveen Sethupathy (https://sethupathy-lab.shinyapps.io/flc_data/), which contained sequenced data related to FLCs. TCGA data related to 6 FLC samples and 50 normal samples could be downloaded from Genomic Data Commons Data Portal (https://portal.gdc.cancer.gov).

Acknowledgements

Preliminary and background studies on effects of extracts of GAGs (heparins, heparan sulfates, hyaluronans) on stem cells were funded by Vesta Therapeutics (Bethesda, MD) to L. Reid. These transitioned into the current studies using defined complexes of synthesized HS-oligosaccharides, prepared by Jian Liu and associates, and paracrine signals; these investigations were funded by the Fibrolamellar Carcinoma Foundation (Greenwich, CT) as an SRA to J. Liu for synthesis of GAGs and to L Reid for the biological studies of the synthesized GAGs and hyaluronans on organoids. Additional funds to J. Liu included NIH grants (HL094463 and HL144970). This work is also supported by GlycoMIP, a National Science Foundation Materials Innovation Platform funded through Cooperative Agreement DMR-1933525.

Since returning to China, W. Zhang has been funded by the Major Program of National Key Research and Development Project (2020YFA0112600), National Natural Science Foundation of China (82270638), Shanghai Pujiang Program (21PJD059), the Key Project of Shanghai Science and Technology Commission (22ZR1451100). Dr. Z. He was funded by the Major Program of National Key Research and Development Projects (2020YFA0112600, 2019YFA0801502), the National Natural Science Foundation of China (82173019, 82203741), The Key Project of Shanghai Science and Technology Commission (17431906600, 22Y11908500), the Program of Shanghai Academic/Technology Research Leader (20XD1434000), the Peak Disciplines (Type IV) of Institutions of Higher Learning in Shanghai, and the Shanghai Engineering Research Center of Stem Cells Translational Medicine (20DZ2255100).

Discounted rates for using core services were provided by the USA federal funding of the cores. These included: a Microscopy Services Laboratory funded by a Cancer Center Core Support grant (P30-CA 016086) –Core directors, formerly Victoria Madden, PhD, and now Pablo Ariel, PhD, and staff, Kristin K. White, MS; a histology core funded by the Center for Gastrointestinal and Biliary Disease Biology (NIDDK Grant: P30 DK034987) with core director, Temitope Keku, PhD and staff, Carolyn Suitt; cores funded by the Lineberger Cancer Center grant (NCI grant # CA016086) including the Carolina Center for Genome Sciences (Katherine Hoadley, PhD, director), and the UNC Center for Bioinformatics (Hemant Kelkar, PhD, director).

Supplementary materials

Supplementary material associated with this article can be found, in

the online version, at doi:10.1016/j.matbio.2023.06.008.

References

- J.R. Craig, R.L. Peters, H.A. Edmondson, M. Omata, Fibrolamellar carcinoma of the liver: a tumor of adolescents and young adults with distinctive clinicopathologic features, Cancer 46 (1980) 372–379.
- [2] M. Torbenson, Fibrolamellar Carcinoma: 2012 Update. Scientifica (Cairo) 743790 (epublication), 15 pages (2012).
- [3] T. Oikawa, et al., Model of fibrolamellar hepatocellular carcinomas reveals striking enrichment in cancer stem cells, Nat. Commun. 6 (2015) 8070.
- [4] W. Zhang et al., in The Liver: Biology and Pathobiology, A. Arias, G. Whitely, A. Wolkoff, Eds. (Wiley Publishers, Hoboken, New Jersey and New York City, NY, 2019), pp. 523–538.
- [5] V. Cardinale, et al., Human duodenal submucosal glands contain a defined stem/ progenitor subpopulation with liver regenerative potency, J. Hepatol. 78 (2023) 165–179.
- [6] V. Cardinale et al., The Biliary Tree: a Reservoir of Multipotent Stem Cells. Nature Reviews. Gastroenterol. Hepatol. 9, 231–240 (2012).
- [7] V. Cardinale, et al., Multipotent stem/progenitor cells in human biliary tree give rise to hepatocytes, cholangiocytes, and pancreatic islets, Hepatology 54 (2011) 2159–2172.
- [8] G. Carpino, et al., Stem/progenitor cell niches involved in hepatic and biliary regeneration. Review, Stem Cells Int. 36580 (2016).
- [9] G. Carpino, et al., Progenitor cell niches in the human pancreatic duct system and associated pancreatic duct glands: an anatomical and immunophenotyping study, J. Anat. 228 (2016) 474–486.
- [10] G. Carpino, et al., Biliary tree stem/progenitor cells in glands of extrahepatic and intrahepatic bile ducts: an anatomical in situ study yielding evidence of maturational lineages. J. Anat. 220 (2012) 186–199.
- [11] G. Carpino, et al., Evidence for multipotent endodermal stem/progenitor cell populations in human gallbladder, J. Hepatol. 60 (2014) 1194–1202.
- [12] E. Schmelzer, et al., Human hepatic stem cells from fetal and postnatal donors, J. Exp. Med. 204 (2007) 1973–1987.
- [13] L. Zhang, N. Theise, M. Chua, L.M. Reid, Human hepatic stem cells and hepatoblasts: symmetry between liver development and liver regeneration, Hepatology 48 (2008) 1598–1607.
- [14] E. Schmelzer, E. Wauthier, L.M. Reid, Phenotypes of pluripotent human hepatic progenitors, Stem Cell 24 (2006) 1852–1858.
- [15] E. Schmelzer, L.M. Reid, Telomerase activity in human hepatic stem cells, hepatoblasts and hepatocytes from neonatal, pediatric, adult and geriatric donors, Eur. J. Gastroenterol. Hepatol. 21 (2009) 1191–1198.
- [16] Y. Wang, et al., Biliary tree stem cells, precursors to pancreatic committed progenitors: evidence for life-long pancreatic organogenesis, Stem Cells 31 (2013) 1966–1979
- [17] D. Overi, et al., Islet regeneration and pancreatic duct glands in human and experimental diabetes, Front. Cell Dev. Biol. (2022).
- [18] T.A. Dinh, et al., MicroRNA-375 suppresses the growth and invasion of fibrolamellar carcinoma, Cell Mol. Gastroenterol. Hepatol. 7 (2019) 803–817.
- [19] T.A. Dinh, et al., Hotspots of aberrant enhancer activity in fibrolamellar carcinoma reveal candidate oncogenic pathways and therapeutic vulnerabilities, Cell Rep. 31 (2020), 107509.
- [20] T.A. Dinh, et al., Comprehensive analysis of the cancer genome atlas reveals a unique gene and non-coding RNA signature of fibrolamellar carcinoma, (Nature) Scientific Reports 7 (2017) 44653.
- [21] J.N. Honeyman, et al., Detection of a Recurrent DNAJB1-PRKACA Chimeric Transcript in Fibrolamellar Hepatocellular Carcinomas, Science 343 (2014) 1010–1014.
- [22] E.R. Kastenhuber, et al., DNAJB1-PRKACA fusion kinase interacts with β-catenin and the liver regenerative response to drive fibrolamellar hepatocellular carcinoma, Proc. Natl. Acad. Sci. USA 114 (2017) 13076–13084.
- [23] G. Lalazar, et al., Identification of novel therapeutic targets for fibrolamellar carcinoma using patient-derived xenografts and direct-from-patient screening, Cancer Discov. 11 (2021) 2544–2563.
- [24] T.A. Dinh, et al., A framework for fibrolamellar carcinoma research and clinical trials, Nature Review-Gastroenterol. Hepatol. 19 (2022) 328–342.
- [25] N.J.C. Narayan, et al., Human liver organoids for disease modeling of fibrolamellar carcinoma, Stem Cell Rep. 17 (2022) 1874–1888.
- [26] T.W. Lu, et al., Structural analyses of the PKA RIIβ holoenzyme containing the oncogenic DnaJB1-PKAc fusion protein reveal protomer asymmetry and fusioninduced allosteric perturbations in fibrolamellar hepatocellular carcinoma, PLoS Biol. 18 (2020), e3001018.
- [27] T.Z. Hirsch, et al., BAP1 mutations define a homogeneous subgroup of hepataocellular carcinoma with fibrolamellar-like features and activated PKA, J. Hepatol. 72 (2020) 924–936.
- [28] H. Cornella, et al., Unique genomic profile of fibrolamellar hepatocellular carcinoma, Gastroenterology 148 (2014) 806–818.
- [29] L. Rüland, et al., Organoid models of fibrolamellar carcinoma mutations reveal hepatocyte transdifferentiation through cooperative BAP1 and PRKAR2A loss, Nat. Commun. 14 (2023) 2377.
- [30] H. Kubota, L.M. Reid, Clonogenic hepatoblasts, common precursors for hepatocytic and biliary lineages, are lacking classical major histocompatibility complex class I antigens, Proc. Natl Acad. Sci. USA 97 (2000) 12132–12137.

[31] C.B. Highley, G.D. Prestwich, J.A. Burdick, Recent advances in hyaluronic acid hydrogels for biomedical applications. Review, Curr. Opin. Biotechnol. 40 (2016) 35–40.

- [32] O.A. Lozoya, et al., Mechanical properties of experimental models of the human liver's stem cell niche microenvironment. I, Biomaterials 32 (2011) 7389–7402.
- [33] H. Sodhi, A. Panitch, Glycosaminoglycans in Tissue Engineering: a Review, Biomolecules 11 (2021).
- [34] D. Vitale, et al., Proteoglycans and glycosaminoglycans as regulators of cancer stem cell function and therapeutic resistance, FEBS J. 286 (2019) 2870–2882.
- [35] A. Hayes, D. Tudor, M. Nowell, B. Caterson, C. Hughes, Unique forms of chondroitin sulfate proteoglycans in stem cell niches, J. Histochem. Cytochem. 56 (2007) 125–138.
- [36] S. Nandadasa, et al., The versican-hyaluronan complex provides an essential extracellular matrix niche for Flk1+ hematoendothelial progenitors, Matrix Biol. 97 (2021) 40–57.
- [37] P.M. Kirkwood, et al., Single-cell RNA sequencing redefines the mesenchymal cell landscape of mouse endometrium, FASEB J. 35 (2021) e21285.
- [38] C. Tao, et al., Chondroitin sulfate enhances the barrier function of basement membrane assembled by heparan sulfate, Development 149 (2022), dev200569.
- [39] A.B. Francisco, et al., Chemical, molecular, and single cell analysis reveal chondroitin sulfate proteoglycan aberrancy in fibrolamellar carcinomas, Cancer Res. Commun. 2 (2022) 663–678.
- [40] J.D. Esko, U. Lindahl, Molecular diversity of heparan sulfate, J. Clin. Invest. 108 (2001) 169–173.
- [41] J. Yang, et al., Construction and Characterization of Heparan Sulfate Heptasaccharide Microarray, Chem. Commun. 53 (2017) 1743–1746.
- [42] Z. Wang, K. Arnold, V.M. Dhurandhare, Y. Xu, L. J, Investigation of the biological functions of heparan sulfate using a chemoenzymatic synthetic approach, RSC Chem. Biol. 2 (2021) 702–712.
- [43] A. Theodoraki, et al., Distinct patterns of heparan sulphate in pancreatic islets suggest novel roles in paracrine islet regulation, Mol. Cell Endocrinol. 399 (2015) 296–310.
- [44] W.C. Lamanna, et al., The heparanome-the enigma of encoding and decoding heparan sulfate sulfation, J. Biotechnol. 129 (2007) 290–307.
- [45] B.I. Ayerst, C.L.R. Merry, A.J. Day, The good the bad and the ugly of glycosaminoglycans in tissue engineering applications, Pharmaceuticals (Basel) 10 (2017) 54.
- [46] D. Xu, K. Arnold, J. Liu, Using structurally defined oligosaccharides to understand the interactions between proteins and heparan sulfate, Curr. Opin. Struct. Biol. 50 (2018) 155–161.
- [47] J.R. Couchman, H. Multhaupt, R.D. Sanderson, Recent insights into cell surface heparan sulphate proteoglycans and cancer (review, ecollection). F1000 Faculty Rev. pii: F1000 Faculty Rev-1541, (2016).
- [48] J.D. Esko, S.B. Selleck, Order out of chaos: assembly of ligand binding sites in heparan sulfate. Annu. Rev. Biochem. 71 (2002) 435–471.
- [49] V.N. Patel, D.L. Pineda, M.P. Hoffman, The function of heparan sulfate during branching morphogenesis. Review, Matrix Biol. 57-58 (2017) 311–323.
- [50] K. Kim, et al., Donor cell type can influence the epigenome and differentiation potential of human induced pluripotent stem cells, Nat. Biotechnol. 29 (2011) 1117–1119.
- [51] J.R. Bishop, M. Schuksz, J.D. Esko, Heparan sulfate proteoglycans fine-tune mammalian physiology, Nature 446 (2007) 1030–1037.
- [52] D. Xu, et al., Heparan sulfate modulates neutrophil and endothelial function in antibacterial innate immunity, Infect. Immun. 83 (2015), 3668-3656.
- [53] O.H. Weiner, M. Zoremba, A.M. Gressner, Gene expression of syndecans and betaglycan in isolated rat liver cells, Cell Tissue Res. 285 (1996) 11–16.
- [54] M. Bernfield, et al., Biology of the syndecans: a family of transmembrane heparan sulfate proteoglycans, Annu. Rev. Cell Biol. 8 (1992) 365–393.
- [55] C.W. Kim, O.A. Goldberger, R.L. Gallo, M. Bernfield, Members of the syndecan family of heparan sulfate proteoglycans are expressed in distinct cell-, tissue-, and development-specific patterns, Mol. Biol. Cell 5 (1994) 797–805.
- [56] N.K. Karamanos, et al., Proteoglycan chemical diversity drives multifunctional cell regulation and therapeutics. Review, Chem. Rev. 118 (2018) 9152–9232.
- [57] J. Filmus, M. Capurro, The role of glypicans in Hedgehog signaling, Matrix Biol. 35 (2014) 248–252.
- [58] S. Zertal-Zidani, A. Bounacer, R. Scharfmann, Regulation of pancreatic endocrine cell differentiation by sulphated proteoglycans, Diabetologia 50 (2007) 585–595.
- [59] F. Zong, et al., Syndecan-1 and FGF-2, but not FGF receptor-1, share a common transport route and co-localize with heparanase in the nuclei of mesenchymal tumor cells, PLoS One 4 (2009) e7346.
- [60] C. Zong, et al., Heparan sulfate microarray reveals that heparan sulfate-protein binding exhibit different ligand requirements, J. Am. Chem. Soc. 139 (2017) 9534–9543.
- [61] V. Kainulainen, H.M. Wang, C. Schick, M. Bernfield, Syndecans, heparan sulfate proteoglycans, maintain the proteolytic balance of acute wound fluids, J. Biol. Chem. 273 (1998) 11563–11569.
- [62] R.J. Holley, K.A. Meade, C.L. Merry, Using embryonic stem cells to understand how glycosaminoglycans regulate differentiation, Biochem. Soc. Trans. 42 (2014) 689–695.
- [63] G.O. Barbosa, M.F. Biancardi, H.F. Carvalho, Heparan sulfate fine-tunes stromalepithelial communication in the prostate gland. Review, Dev. Dyn. 250 (2021) 618–628.
- [64] R. Liu, et al., Chemoenzymatic design of heparan sulfate oligosaccharides, J. Biol. Chem. 285 (2010) 34240–34249.
- [65] J. Liu, L. RJ, Chemoenzymatic synthesis of heparan sulfate and heparin. Review, Nat. Prod. Rep. 31 (2014) 1676–1685.

- [66] T. Oikawa, et al., Sall4 regulates cell fate decision in fetal hepatic stem/ progenitor cells, Gastroenterology 136 (2009) 1000–1011.
- [67] H. Kubota, R. Storm, and L.M. Reid. Variant Forms of alpha-Fetoprotein transcripts expressed in human hematopoietic progenitors. Implications for their developmenetal potential towards endoderm, J. Biol. Chem. 277 (2002) 27629–27635.
- [68] T. Oikawa, et al., SALL4, a stem cell biomarker in liver cancers, Hepatology 57 (2013) 1469–1483.
- [69] V. Cardinale, et al., Profiles of cancer stem cell subpopulations in cholangiocarcinomas, Am. J. Pathol. 185 (2015) 1724–1739.
- [70] V. Cardinale, et al., Cholangiocarcinomas: new insights from the discovery of stem cell niches in peribiliary glands of the biliary tree, Adv. Hepatol. 2014 (2014) 1-10
- [71] H.G. Woo, et al., Association of TP53 mutations with stem cell-like gene expression and survival of patients with hepatocellular carcinoma, Gastroenterology 140 (2011) 1063–1070.
- [72] K. Sato, et al., Organoids and spheroids as models for studying cholestatic liver injury and cholangiocarcinoma.review, Hepatology 74 (2021) 491–502.
- [73] G.K.L. Chan, et al., Oncogenic PKA signaling increases c-MYC protein expression through multiple targetable mechanisms, Elife 12 (2023) e69521.
- [74] Y. Wang, et al., Lineage restriction of hepatic stem cells to mature fates is made efficient by tissue-specific biomatrix scaffolds, Hepatology 53 (2011) 293–305.
- [75] R.C. Gessner, et al., New ultrasound perfusion imaging techniques enable functional assessment of biomatrix scaffolds for human organoid formation, Biomaterials 34 (2013) 9341–9351.
- [76] Y. Wang, et al., Lineage-dependent epithelial-mesenchymal paracrine signals dictate growth versus differentiation of human hepatic stem cells to adult fates, Hepatology 52 (2010) 1443–1454.
- [77] H. Kubota, H. Yao, L.M. Reid, Identification and characterization of vitamin Astoring cells in fetal liver, Stem Cell 25 (2007) 2339–2349.
- [78] A.B. Francisco, et al., Chemical, molecular, and single-nucleus analysis reveal chondroitin sulfate proteoglycan aberrancy in fibrolamellar carcinoma, Cancer Res. Commun. 2 (2022) 663–678.
- [79] J.M. Granja, et al., ArchR is a scalable software package for integrative single-cell chromatin accessibility analysis, Nat. Genet. 53 (2021) 403–411.
- [80] A.R. Rezaie, H. Giri, Anticoagulant and signaling functions of antithrombin, J. Thromb. Haemost. 18 (2020) 3142–3153.
- [81] N. Hassan, J. Efing, L. Kiesel, G. Bendas, M. Götte, The tissue factor pathway in cancer: overview and role of heparan sulfate proteoglycans. Review, Cancers (Basel) 15 (2023) 1524.
- [82] A.I.S. Sobczak, S. Pitt, A. Stewart, Glycosaminoglycan neutralization in coagulation control, Arterioscler. Thromb. Vasc. Biol. 38 (2018) 1258–1270.
- [83] D.C. Spray, et al., Proteoglycans and glycosaminoglycans induce gap junction synthesis and function in primary liver cultures, J. Cell Biol. 105 (1987) 541–551.
- [84] M. Lyon, J.A. Deakin, J.T. Gallagher, The mode of action of heparan and dermatan sulfates in the regulation of hepatocyte growth factor/scatter factor, J. Biol. Chem. 277 (2002) 1040–1046.
- [85] A. Amara, et al., Stromal cell-derived factor-1a associates with heparan sulfates through the first B-strand of the chemokine, J. Biol. Chem. 274 (1999) 23916–23925.
- [86] G. Chen, et al., α-Klotho is a non-enzymatic molecular scaffold for FGF23 hormone signalling, Nature 553 (2018) 461–466.
- [87] M.D. Stewart, R.D. Sanderson, Heparan sulfate in the nucleus and its control of cellular functions, a mini-review, Matrix Biol. 35 (2014) 56–59.
- [88] M.D. Stewart, V.C. Ramani, R.D. Sanderson, Shed syndecan-1 translocates to the nucleus of cells delivering growth factors and Inhibiting histone acetylation, a novel mechanism of tumor-host cross talk, J. Biol. Chem. 290 (2014) 941–949.
- [89] V.N. Patel, et al., Hs3st3-modified heparan sulfate controls KIT+ progenitor expansion by regulating 3-O-sulfotransferases, Dev. Cell 29 (2014) 662–673.
- [90] J. Liu, A.F. Moon, J. Sheng, L.C. Pedersen, Understanding the substrate specificity of the heparan sulfate sulfotransferases by a combined synthetic crystallographic approach, Curr. Opin. Struct. Biol. 22 (2012) 550–557.
- [91] V. Cardinale, et al., Human duodenal submucosal glands contain a defined stem/ progenitor subpopulation with liver-specific regenerative potential, J. Hepatol. (2022)
- [92] M.E. Furth et al., in The Stem Cells Handbook, 2nd Edition, S. Sell, Ed. (Springer Science Publishers, NYC, 2013), pp. 75–126.
- [93] M. Martín-Alonso, et al., Smooth muscle-specific MMP17 (MT4-MMP) regulates the intestinal stem cell niche and regeneration after damage, Nat. Commun. 12 (2021) 6741.
- [94] Q. Chen, et al., Long non-coding RNA ERICH3-AS1 is an unfavorable prognostic factor for gastric cancer, PeerJ 8 (2020) e8050.
- [95] E.A. Turley, P.W. Noble, L.Y. Bourguignon, Signaling properties of hyaluronan receptors, J. Biol. Chem. 277 (2002) 4589–4592.
- [96] Y. Yan, X. Zuo, D. Wei, Concise review: emerging role of CD44 in cancer stem cells: a promising biomarker and therapeutic target, Stem Cells Transl Med 4 (2015) 1033–1043.
- [97] I. Morath, T.N. Hartmann, V. Orian-Rousseau, CD44: more than a mere stem cell marker, Int. J. Biochem. Cell Biol. 81 (2016) 166–173.
- [98] D.S. Schmidt, P. Klingbell, M. Schnolzer, M. Zoller, CD44 variant isoforms associate with tetraspanins and EpCAM, Exp. Cell Res. 297 (2004) 329–347.
- [99] D. Naot, R. Sionov, I.S. D, CD44: structure, function, and association with the malignant process, Adv. Cancer Res. 71 (1997) 241–319.

[100] H. Hu, et al., Long-term expansion of functional mouse and human hepatocytes as 3D organoids, Cell 175 (2018).

- [101] M. Huch, et al., Long-term culture of genome-stable bipotent stem cells from adult human liver, Cell 160 (2015) 299–312.
- [102] M. Huch, S.F. Boj, H. Clevers, Lgr5(+) liver stem cells, hepatic organoids and regenerative medicine, Regen. Med. 8 (2013) 385–387.
- [103] D.F. Kaluthantrige, M. Huch, Organoids, where we stand and where we go. Review. Trends Mol. Med.. 27, 416–418 (2021).
- [104] A. Marsee, et al., Building consensus on definition and nomenclature of hepatic, pancreatic, and biliary organoids, Cell Stem Cell 28 (2021) 816–832.
- [105] G. Amaddeo, C. Guichard, S. Imbeaud, J. Zucman-Rossi, Next-generation sequencing identified new oncogenes and tumor suppressor genes in human hepatic tumors, Oncoimmunology 1 (2012) 1612–1613.
- [106] E. Olsson, et al., CD44 isoforms are heterogeneously expressed in breast cancer and correlate with tumor subtypes and cancer stem cell markers, BMC Cancer 11 (2011) 418.
- [107] J.T. Gallagher, J.E. Turnbull, Heparan sulphate in the binding and activation of basic fibroblast growth factor, Glycobiology 2 (1992) 523–528.
- [108] M. Lyon, J.T. Gallagher, Purification and partial characterization of the major cell-associated heparan sulphate proteoglycan of rat liver, Biochem. J. 273 (1991) 415–422.
- [109] M. Lyon, G. Rushton, J.A. Askari, M.J. Humphries, J.T. Gallagher, Elucidation of the structural features of heparan sulfate important for interaction with the Hep-2 domain of fibronectin, J. Biol. Chem. 275 (2000) 4599–4606.
- [110] M. Lyon, J.A. Deakin, K. Mizuno, T. Nakamura, J.T. Gallagher, Interaction of hepatocyte growth factor with heparan sulfate, J. Biol. Chem. 269 (1994) 11216–11223.
- [111] M. Lyon, J.A. Deakin, J.T. Gallagher, Liver heparan sulfate structure. A novel molecular design, J. Biol. Chem. 269 (1994) 11208–11215.
- [112] L. Chen, R.D. Sanderson, Heparanase regulates levels of syndecan-1 in the nucleus, PLoS One 4 (2009) e4947.
- [113] B. Thacker, D. Xu, R. Lawrence, J. Esko, Heparan sulfate 3-O-sulfation: a rare modification in search of a function, Matrix Biol. 35 (2014) 60–72.
- [114] D. Shukla, et al., A novel role for 3-O-sulfated heparan sulfate in herpes simplex virus 1 entry, Cell 99 (1999) 13–22.
- [115] B.E. Thacker, et al., Expanding the 3-o-sulfate proteome-enhanced binding of neuropilin-1 to 3-o-sulfated heparan sulfate modulates its activity, ACS Chem. Biol. 11 (2016) 971–980.
- [116] R. Karlsson, et al., Dissection structure-function of 3-0 sulfated heparin and engineered heparan sulfates, Sci. Adv. 7 (2021) 1–13.
- [117] L.M. Reid, P. Sethupathy, The DNAJB1-PRKACA chimera: candidate biomarker and therapeutic target for fibrolamellar carcinomas, Hepatology (Hepatology Elsewhere) 63 (2015) 662–663.
- [118] R. Gulati, et al., Beta-catenin-cancer-enhancing genomic regions axis is involved in the development of hepatoblastomas and fibrolamellar carcinomas, Hepatol. Commun. 6 (2022) 2950–2963.
- [119] X. Shu, Y. Liu, F. Palumbo, Y. Luo, G. Prestwich, In situ crosslinkable hyaluronan hydrogels for tissue engineering, Biomaterials 25 (2004) 1339–1348.
- [120] W. Zhang, et al., Patch grafting, strategies for transplantation of organoids into solid organs such as liver, Biomaterials 277 (2021) 1–10.
- [121] E. Wauthier, et al., Hepatic stem cells and hepatoblasts: identification, isolation and ex vivo maintenance, Methods Cell Biol. 86 (2008) 137–225.
- [122] G. Carpino, et al., Peribiliary gland niche participates in biliary tree regeneration in mouse and in human primary sclerosing cholangitis, Hepatology 7 (2020) 972–989
- [123] R. Turner, et al., Cryopreservation of human hepatic stem/progenitor cells. Importance of protection of adhesion mechanisms, Cell Transplant 21 (2012) 2257–2266.
- [124] L. Nevi, et al., Cryopreservation protocol for human biliary tree stem/progenitors, hepatic and pancreatic precursors, Sci. Rep. 7 (2017) 6080.
- [125] K.R. Kirker, G.D. Prestwich, Physical properties of glycosaminoglycan hydrogels, J. Polymer Sci. B: Polymer Phys. 42 (2004) 4344–4356.
- [126] E.L. Chaikof, et al., Biomaterials and scaffolds in reparative medicine, Ann. N. Y. Acad. Sci. 961 (2002) 96–105.
- [127] Y. Liu, X.Z. Shu, G.D. Prestwich, Biocompatibility and stability of disulfidecrosslinked hyaluronan films, Biomatierals 26 (2005) 4737–4746.
- [128] X.Z. Shu, G.D. Prestwich, in Chemistry and Biology of Hyaluronan, H. Garg, C. Hales, Eds. (Elsevier Press, Amsterdam, 2004), pp. 475–504.
- [129] G.D. Prestwich, D.M. Marecak, J.F. Marecak, K.P. Vercruysse, M.R. Ziebell, Controlled chemical modification of hyaluronic acid: synthesis, applications, and biodegradation of hydrazide derivatives, J. Controlled Release 53 (1998) 93–103.
- [130] J.L. Vanderhooft, M. Alcoutlabi, J.J. Magda, G.D. Prestwich, Rheological properties of cross-linked hyaluronan-gelatin hydrogels for tissue engineering, Macromol Biosci 9 (2009) 20–28.
- [131] W. Zhang, et al., Patch grafting of organoids of stem/progenitors into solid organs can correct genetic-based disease states, Biomaterials 288 (2022), 121647.
- [132] Y. Hao, et al., Integrated analysis of multimodal single-cell data, Cell 184 (2021) 3573–3587, e3529.
- [133] Y. Xu, et al., Homogeneous and reversible low-molecular weight heparins with reversible anticoagulant activity, Nat. Chem. Biol. 10 (2014) 248–250.
- [134] P. Hsieh, Y. Xu, D.A. Keire, J. Liu, Chemoenzymatic synthesis and structural characterization of 2-O-sulfated glucuronic acid containing heparan sulfate hexasaccharides, Glycobiology 24 (2014) 681–692.